Numerical Study of Flat Plate Solar Air Heaters With and Without Fins

Ayşegül Gazioğlu

Submitted to the
Institute of Graduate Studies and Research
in partial fulfillment of the requirements for the degree of

Master of Science
in
Mechanical Engineering

Eastern Mediterranean University
September 2021
Gazimağusa, North Cyprus

Approval of the Institute of Graduate Studies and Research

Prof. Dr. Ali Hakan Ulusoy
Director

I certify that this thesis satisfies all the requirements as a thesis for the degree of Master of Science in Mechanical Engineering.

Prof. Dr. Hasan Hacışevki
Chair, Department of Mechanical Engineering

We certify that we have read this thesis and that in our opinion it is fully adequate in scope and quality as a thesis for the degree of Master of Science in Mechanical Engineering.

Prof. Dr. Hasan Hacışevki
Supervisor

Examining Committee

1. Prof. Dr. Hasan Hacışevki

2. Assoc. Prof. Dr. Hüseyin Çamur

3. Assoc. Prof. Dr. Murat Özdenefe

ABSTRACT

Solar air heaters are devices which utilize absorbed solar energy by transferring heat to the air passing through air channels. Present study investigates the performance enhancement of a conventional solar air heater by assigning rectangular fins to the bottom plate. The impact of the assigned fins are examined by comparing the finned flat plate solar air heater with a standard flat plate solar air heater without fins, over a relevant range of air mass flow rate and solar irradiance values. The mathematical model built is numerically solved on MATLAB-R2020b. The results indicate that installation of fins boosts the performance of flat plate solar air collectors significantly. Use of fins in the solar air collector results in increased heat removal factor, useful energy gain, as well as collector efficiency values, and lowered the heat loss coefficients. The collector efficiency improves from 47.78% to 61.32%, with the addition of fins, at mass flow rate 0.01 kg/s and solar irradiance 1000 W/m^2. The maximum collector efficiency 61.46% of the finned air collector is achieved at air mass flow rate 0.01 kg/s and solar irradiance 1200 W/m^2. The findings of the study indicate that the finned solar air heater works the most efficiently at lower air mass flow rates and greater solar irradiances.

Keywords: solar air heaters, solar energy, heat transfer

ÖZ

Güneş enerjili hava ısıtıcıları, güneş ışınlarından emilen güneş enerjisini, hava kanalından akan havayı ısıtmak için kullanan cihazlardır. Mevcut çalışma, konvansiyonel düz plaka güneş enerjili hava ısıtıcısına dikdörtgen kanatçık ekleminin, performans artışı üzerindeki etkisini incelemektedir. Çalışma, kanatçıklı ve kanatçıksız düz plaka güneş enerjili hava ısıtıcı performanslarını ilgili hava debisi ve güneş ışınımı değer aralıklarında karşılaştırmaktadır. Geliştirilmiş matematiksel model MATLAB-R2020b yazılımında çözülmüştür. Varılan sonuçlar, kanatçık ekleminin düz plaka güneş enerjili hava ısıtıcılarında performans artışına neden olduğunu göstermektedir. Kanatçıklar, ısı giderme faktörü, kullanılabilir enerji kazancı ve verimlilik değerlerinde artışa sebep olurken, ısı kaybı katsayılarında düşüşe neden olmaktadır. Hava debisi 0.01 kg/s ve güneş ışınımı 1000 W/m^2 iken, kanatçıklı güneş enerjili hava ısıtıcısı konvansiyonel güneş enerjili hava ısıtıcısı ile karşılaştırıldığında, kanatçıkların verimlilik değerini %47.78'den %61.32'e yükselttiği görülmektedir. Kanatçıklı güneş enerjili ısıtıcısı için maksimum verimlilik, hava debisi 0.01 kg/s ve güneş ışınımı 1200 W/m^2 iken %61.46 olarak elde edilmektedir. Elde edilen sonuçlar ışığında, kanatçıklı düz plaka güneş enerjili ısıtıcılarının düşük hava debileri ve yüksek güneş ışınımlarında en verimli çalıştıkları anlaşılmaktadır.

Anahtar kelimeler: Güneş enerjili hava ısıtıcıları, güneş enerjisi, ısı transferi

ACKNOWLEDGEMENT

First and foremost, I wish to express my most sincere gratitude and appreciation to Prof. Dr. Hasan HACIŞEVKİ, not only for his guidance and help throughout the development of the thesis, but most importantly for his assistance and encouragement throughout the course of my study, from start to finish. His continuous support for me is something that I will forever cherish and be grateful for. His supportive nature, valuable experiences and infinite wisdom have tremendously inspired me to strive to be a better student. For that, I will always be thankful.

I would like to wish my sincere thanks to Prof. Dr. Uğur ATİKOL, for sparking my newly found interest in the area of renewable energy. His encouragement and enthusiasm to push for novel ideas is truly inspiring.

I also would like to express my deepest thanks to Assoc. Prof. Dr. Qasım ZEESHAN. Taking his classes in my very first semester was definitely one of the highlights of my time in EMU. I will forever be grateful for his encouragement and wisdom, and I truly admire his enthusiasm for teaching.

Finally, I would like to wish my most sincere thanks to my family for standing by my side at all times, supporting me throughout whichever journey I take. I am forever indebted to them.

TABLE OF CONTENTS

LIST OF TABLES

LIST OF FIGURES

LIST OF SYMBOLS

A_c	Collector surface area (m^2)
A_f	Total surface area of the fins (m^2)
c_p	Specific heat of air when pressure is kept as constant (J/kgK)
D_h	Duct (channel) hydraulic diameter (m)
d_{pg}	Distance between absorber plate and glass cover (m)
ε_b	Emissivity of bottom plate
ε_g	Emissivity of glass cover
ε_p	Emissivity of absorber plate
F'	Collector efficiency factor
F_R	Heat removal factor of collector
$h_{c,b-f}$	Convection heat transfer coefficient between bottom plate to flowing air (working medium) (W/m^2K)
$h_{c,p-f}$	Convection heat transfer coefficient of absorber plate to the working medium (W/m^2K)
$h_{c,p-g}$	Convective heat transfer coefficient between the absorber plate and the glass cover (W/m^2K)
h_c	Convective heat transfer coefficient (W/m^2K)
$h_{r,g-a}$	Radiation heat transfer coefficient from glass cover to the ambient (W/m^2K)
$h_{r,p-b}$	Radiation heat transfer coefficient between absorber plate and bottom plate (W/m^2K)

$h_{r,p-g}$	Radiation heat transfer coefficient from the absorber plate to glass cover (W/m^{2}K)
h_r	Radiant heat transfer coefficient (W/m^{2}K)
h_w	Heat transfer coefficient of wind (W/m^{2}K)
k_a	Air thermal conductivity coefficient (W/mK)
k_f	Thermal conductivity of fins (W/mK)
k_s	Insulation thermal conductivity (W/mK)
k_{Tf}	Convective heat transfer coefficient of airflow (W/m^{2}K)
L_c	Length of collector (m)
L_t	Height of fins(m)
$\dot{m}$	Mass flow rate of air (kg/s)
N_g	Number of glass covers
N_t	Number of fins attached
N_{ti}	Number of fins on front row
Q_u	Useful energy gain (W)
T_a	Ambient temperature (K)
T_b	Temperature of bottom plate (K)
T_f	Temperature of flowing air (K)
t_f	Thickness of fins (m)
T_g	Temperature of glass cover (K)
T_i	Incoming (inlet) air flow temperature (K)
T_O	Outlet air temperature (K)
T_p	Temperature of absorber plate (K)
U_b	Bottom heat loss coefficient (W/m^{2}K)

U_L	Overall heat loss coefficient (W/m^{2}K)
U_t	Top heat loss coefficient (W/m^{2}K)
V_f	Velocity of flowing air (m/s)
W_t	Width of fins (m)
α_g	Absorptivity of glass cover
α_p	Absorptivity of absorber plate
δ_c	Thickness of collector (m)
δ_s	Thickness of insulator (m)
η_f	Fin efficiency
ρ_a	Air density (kg/m^3)
τ_g	Transmittivity of glass cover
ΔT	Temperature difference between outlet and inlet air (K)
B	Width of the air channel (m)
g	Gravitational acceleration (m/s^2)
H	Depth of duct (channel) (m)
I	Solar irradiance (W/m^2)
Nu	Nusselt number
Pr	Prandtl number
Ra	Rayleigh number
Re	Reynolds number
S	Solar radiation absorbed (W/m^2)
T	Mean sum of absorber plate and glass cover temperature (K)
V	Wind velocity (m/s)
η	Collector efficiency

θ	Tilt angle of the collector (degrees)
μ	Dynamic viscosity kg/m s
ν	Kinematic viscosity of flowing air m^2/s
σ	Stefan-Boltzmann constant (W/m^2K^4)
$\tau\alpha$	Transmitted absorption coefficient
ϕ	Dimensionless quantity

Chapter 1

INTRODUCTION

1.1 Solar Energy

In the recent years, the energy demand has increased immensely. The concern for environmental pollution and the shortage of fossil fuel energy resources have heightened with the growing demands. As a result, engineers and scientists have turned to concentrate on the utilization of renewable energy sources. It does not come as a surprise that solar energy appears to be one of the most advantageous energy source in the renewable energy sector, due to its free availability and cleanliness in comparison with other various energy sources.

1.2 Solar Air Heaters

A solar air heater is a device which utilizes solar energy absorbed from the sun rays, and transfers the absorbed heat to the flowing air in the air channels. A typical solar air heater is made up of a glass cover, an absorber plate and a bottom plate. It is common practice to instal a fan in order to force air flow across the heated plates. For such cases, forced convection heat transfer takes place. For the cases where a fan is not used, convective heat transfer takes place naturally due to buoyancy forces. This is known as natural convection. Solar air heaters are utilized in a broad range of applications. These include crop drying, air heating, space heating, dry cleaning as well as other agricultural and industrial applications. [1] In the agriculture industry, solar air heaters are used to dry crops such as tomatoes, apricots, corn, tea and etc. Additionally, solar air heaters are beneficial in the maintenance of high sanitary

standards in the crop drying processes, as they lower the possibilities of the crops getting contaminated with dust and bacteria. The general working principle of solar air heaters used for crop drying purposes is that the heated air exiting device hovers over the crops and reduces their moisture content. [2]

As useful as the solar air heaters currently used in the industry may be, there is still a lot of room for improvement and research for solar air heater technologies. The limitations of solar air collectors is that they tend to have low efficiencies. Hence, researches continue to investigate different approaches and design configurations to overcome these limitations.

1.3 Aims and Targets of The Present Study

This study aims to analyse the impact installation of fins have on the performance of standard flat plate solar air collectors. Two sorts of solar air heaters are looked into in this study; flat plate solar air heater with assigned fins and flat plate solar air heater without fins. The study aims to acquire findings about how the addition of fins to the bottom plate of a solar air heater affects overall heat loss, heat removal factor, useful energy obtained by the collector, exiting (can interchangeably be called outlet) air temperature and collector efficiency. The performance of the solar air collectors of conventional type and with assigned fins are to be tested over varying mass flow rates and solar insolation values.

Chapter 2

LITERATURE REVIEW

2.1 Reviewing Solar Air Heaters

Although solar air heaters are not made use of as much as solar water heating devices are, they still prove to be very advantageous for a number of reasons. As opposed to solar water heating systems, solar air heaters are not concerned with issues such as freezing of air, serious leakage of air and corrosion in mixed metal systems. [3] However, solar air heaters also have their drawbacks. Solar air heaters are limited in their working hours since solar energy is only available during day time. In addition, the manufacturing costs of panels can be relatively costly.

Heat transfer occurs in solar air heaters through convection and radiation. The collector materials absorb solar radiation, and a fan forces the air to flow over the heated surfaces. Convective heat transfer takes place as the air moves over the heated solid surfaces.

There may be variances in the absorber plates used in solar air heaters. Especially in countries with hotter climates such as Cyprus, Iran, India and many other, it is quite common to build an in-house solar air heater, as solar energy is available in abundance in such countries. Materials such as cola cans and polymers are used in the absorber plate sections of the in-house solar heaters. Further, solar air heaters can be categorized with regard to the types of absorber media they have; porous and non – porous. Porous

absorber plates constitute of materials such as matrix and metal sponge wire mesh, and non-porous types are typically made of flat plates and sheets which are V-corrugated. [4] Additionally, solar air collectors can further be categorized according to different absorber plate shapes.

The most common shapes for absorber plates can be listed as:

- Roughened surfaces
- Corrugated sheets
- Honey comb
- Wire mesh
- Fins and extended surfaces
- Baffles
- Fins and baffles combined.

The aforementioned shapes aid in increasing the useful energy gain and thermal efficiency, all while reducing heat losses. [4]

2.2 Reviewing Previous Researches and Experimentations

Many investigations have been executed by a number of researchers in an effort to achieve more desirable performances out of solar air heaters. In the previous chapter, it was mentioned that the said devices are widely used in agriculture. Womac et al. (1985) tested how suspended-plate solar air heaters established in farms of Tennessee performed in terms of thermal analysis. The said solar air heaters were used for crop and grain drying. It was found that the solar air heaters investigated scored thermal efficiencies 50% -70%. [1] Koyuncu (2006) also analysed the usage of solar air collectors of flat plate type for agricultural purposes. [2]

Moreover, Chabane et al. (2013) examined the thermal performance of flat plate solar air collectors with mass flow rates of the magnitude 0.012 kg/s and 0.016 kg/s. The study evaluated that the thermal efficiencies can be enhanced with higher mass flow rates.[5]

Since flat plates are one of the earliest designs of all solar air heater types, many studies have been carried out about them. With the motivation to improve the operation of solar air heaters, researchers started to test difference design configurations, such as adding fins, baffles or the combination of fin and baffles to flat plate solar collectors as well as using roughened surfaces, wire mesh, honeycomb structures and etc.

Yeh et al. (1998) looked into the impacts of baffles on the collector efficiencies. They installed baffles with fins and without fins and kept the collector dimensions constant. The results showed that installing baffles led to a boost in the collector efficiencies.[6] Gopi (2017) examined the effects of attaching cylindrical fins on the operation of solar air collectors. In the study it was distinguished that assigning cylindrical fins contributes to a boost in the temperature of outlet (exiting) air and the system efficiency of the heater.[7] Daliran and Ajabschirchi (2018) carried out an experimental alongside a numerical investigation evaluating flat plate solar heaters with rectangular fins. They have seen that the finned air heater achieved an efficiency value of 51%, meanwhile 30% was achieved for conventional solar air heater.[8]

The variations on the operational behaviour of single pass solar air heaters on account of the effects of fins and baffles were analysed by Mohammadi and Sabzpooshani (2013). [9] It was concluded that fins and baffles led to a rise in the exiting air

temperatures and collector efficiency. It was also found that using fins and baffles that are wider lowered the effective efficiency.

Kumar and Chand (2017) examined the improvement in the performance of solar air heaters which were assigned with herringbone corrugated fins. In their study they found that there was a jump in the thermal efficiencies of solar air collector at fin pitch 0.025 m and a set mass flow rate 0.026 kg/s. This jumps was from 36.2 % to 56.6%. [10]

Naphon (2005) assigned longitudinal fins to double pass solar air heaters. It was observed that increasing the fin heights and the number of fins enhanced the thermal efficiency. [11] It is also worth to mention that in the studies of solar heaters, the most common range used for mass flow rates is 0.01-0.12 kg/s when testing for performance.

Last but not least, Rai et al. (2017) looked into the effects on offset fins attached to the bottom of the absorber plate on the thermal and thermohydraulic efficiencies of solar air heaters, with a varying of system configurations, for instance, fin spacing, fin height and air mass flow rate. It was found that the thermohydraulic efficiency was maximized at a particular mass flow rate and beyond point the thermohydraulic efficiency decreased very sharply. It was also found that by the assigning offset fins on the bottom plate at lower mass flow rates, the thermal efficiency was enhanced to 106.9% and the thermohydraulic efficiency rose to 67.38%. [13]

Chapter 3

MATERIALS AND METHODS

3.1 Structural Arrangement of The Solar Air Heater System

Two sorts of flat plate solar air heater designs are evaluated in this study; finned and without fins. The materials and structures of the hypothetical solar air heater systems assumed in this study were selected similar to that of Daliran et al. [8]. Both solar air collectors consist of the following parts; a single typical glass cover, an absorber plate and a bottom plate, as well as a fan to force air flow. The only different design configuration between the two systems is the inclusion of fins to the bottom plate of the finned solar air collector. The thickness of each component of the solar air heater without fins and the distance between them is visually presented in Figure 1. The bottom plate illustrated in Figure 1 is that of the solar air heater without fins. The bottom plate considered for the finned solar air heater is presented in Figure 2. Figure 3 presents a view of the angle in which the fins are attached to the bottom plate. It should be stated that the dimensions of the glass cover and the absorber plate, as well as the distance between them is the same for both solar air heaters considered in the study. The dimensions of the bottom plate is also the same, with the difference that fins are attached to the bottom plate of the finned solar air collector.

Iron sheets are the materials of the absorber plate and back plate (bottom plate). The fins attached to the finned solar air collector are made of galvanized iron. Moreover, each collector has a surface area of 1 m^2 and the collector length is 1.25 m. Each glass

cover has a thickness of 0.004 m. The glass cover and the absorber plate are 0.03 m far from each other. The absorber plate and the bottom plate is 0.04 m apart. The absorber plate is 0.00115 m thick and is made of iron sheet. The bottom plate is 0.009 m thick. The collector tilt angle is 31 degrees. The air channel of the collector has a height and width of 0.04 m and 0.8 m, respectively.

For the finned solar air heater, there are 80 fins attached to the bottom plate in total, with 8 fins per row. The thickness of each fin is 0.0007 m. Each fin has a height and width of 0.05 m and 0.035 m, respectively. The fins are arranged in the following manner; the lateral spacing between two adjacent fins is 0.03 m, and the longitudinal spacing between the fins is 0.1 m. The angle in which the fins are placed is 40 degrees. Moreover, the back part of the collector is insulated to minimize any further heat losses.

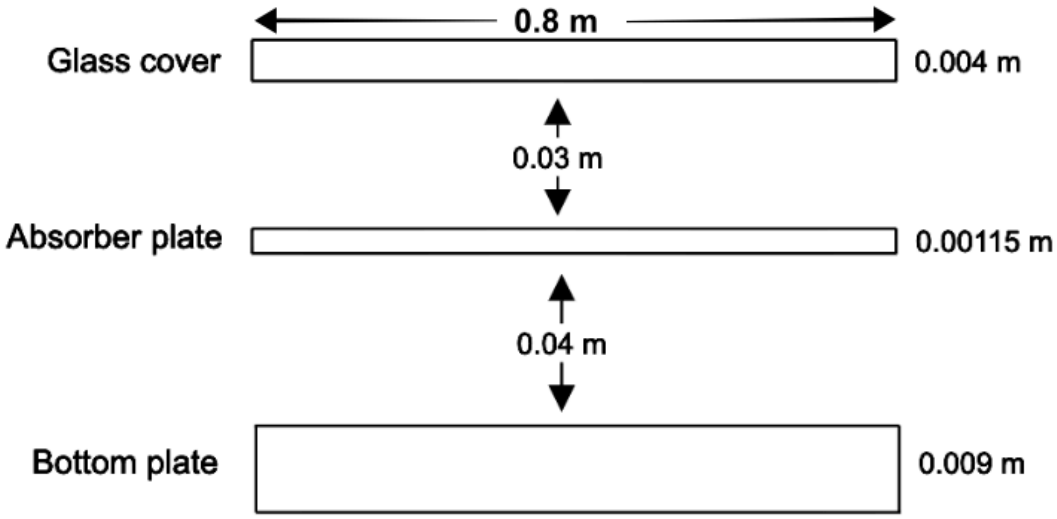

Figure 1: Thickness of the components of the solar air heater without fins and the distance between them shown from front side view. [8] (Drawing not to scale.)

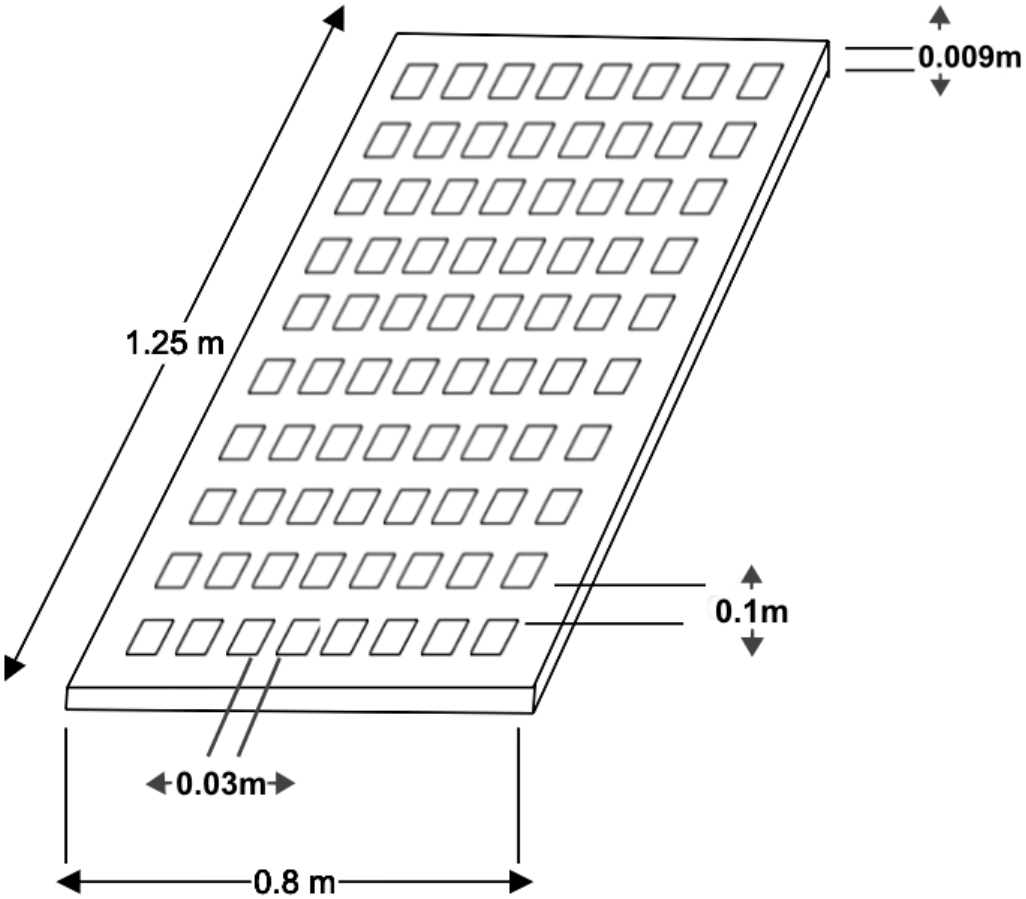

Figure 2: Dimensions of the bottom plate of the finned solar air heater. [8] (Drawing not to scale, fins attached at angle of 40 degrees.)

3.2 Mathematical Model of The Studied Flat Plate Solar Air Heaters

A mathematical model was developed and presented for the hypothetical solar air systems assumed in this study. The model considers the properties of the structure as well as the environmental properties.

3.2.1 Assumptions

The numerical analysis was carried out on the basis of the listed assumptions [12]:

i. The operation conditions are in steady state.

ii. The heat flows in one dimension and is in the same direction as the flow.

iii. The edge heat losses are negligible.

3.2.2 Energy Equilibrium Equations

The energy equilibrium equations were written for the glass cover, absorber and bottom plate (back plate), and the working medium (flowing air), at steady state, respectively. [8]

Glass cover:

$$\alpha_g I + \left(h_{c,p-g} + h_{r,p-g}\right)\left(T_p - T_g\right) = (h_w + h_{r,g-a})(T_g - T_a) \quad (1)$$

Absorber plate:

$$\alpha_p \tau_g \, I = \left(h_{c,p-g} + h_{r,p-g}\right)\left(T_p - T_g\right) + h_{r,p-b}\left(T_p - T_b\right) + h_{c,p-f}(T_p - T_f) \quad (2)$$

Bottom plate:

$$h_{r,p-b}\left(T_p - T_b\right) = \phi \, h_{c,b-f}\left(T_b - T_f\right) + U_b(T_b - T_a) \quad (3)$$

Working medium (flowing air):

$$\dot{m} \, c_p\left(T_f - T_i\right) = \, h_{c,p-f}\left(T_p - T_f\right) + \phi h_{c,b-f}(T_b - T_f) \quad (4)$$

3.2.3 Temperatures of Components

Equations (1) –(4) were rearranged to obtain expressions for the of the glass cover, absorber plate, bottom plate as well as the working medium (flowing fluid) temperatures.

Glass cover:

$$T_g = \frac{\alpha_g I + T_p\left(h_{c,p-g} + h_{r,p-g}\right) + T_a(h_w + h_{r,g-a})}{h_{c,p-g} + h_{r,p-g} + h_w + h_{r,g-a}} \quad (5)$$

Absorber plate:

$$T_p = \frac{\alpha_g \tau_p \, I + T_g\left(h_{c,p-g} + h_{r,p-g}\right) + T_b(h_{r,p-b}) + T_f(h_{c,p-f})}{h_{c,p-g} + h_{r,p-g} + h_{r,p-b} + h_{c,p-f}} \quad (6)$$

Bottom plate:

$$T_b = \frac{T_p\left(h_{r,p-b}\right) + T_f \phi (h_{c,b-f}) + T_a U_b}{h_{r,p-b} + \phi h_{c,b-f} + U_b} \quad (7)$$

Working medium (flowing air):

$$T_f = \frac{T_i \dot{m}\, c_p + T_p(h_{c,p-f}) + T_b \phi (h_{c,b-f})}{\dot{m}\, c_p + h_{c,p-f} + \phi h_{c,b-f}} \quad (8)$$

3.2.4 Calculation of Heat Transfer Coefficients

There is heat transfer that occurs between the glass cover and the ambience due to convection. The heat transfer coefficient due to convection between the glass cover and the ambient is shown by the symbol $h_{c,g-a}$. Considering the fact that solar air heater systems are installed in outdoor environments, we could then state that the wind heat transfer coefficient, h_w is the equivalent of $h_{c,g-a}$. [8] The following equation illustrates the relation of the two heat transfer coefficients, where V is the wind velocity.

$$h_{c,g-a} = h_w = \frac{8.6(V)^{0.6}}{L_c^{0.4}} \quad (9)$$

The radiation heat transfer coefficients from the glass cover to the ambient is demonstrated by equation (10) [9].

$$h_{r,g-a} = \mathcal{E}_g\, \sigma\, (T_g + T_a)(\, (T_g^2 + T_a^2) \quad (10)$$

The heat transfer coefficient due to radiation from the absorber plate to the glass cover is found from equation (11) as follows [13].

$$h_{r,p-g} = \frac{\sigma\, (T_p + T_g)(T_p^2 + T_g^2)}{\left(\frac{1}{\varepsilon_p}\right) + \left(\frac{1}{\varepsilon_g}\right) - 1} \quad (11)$$

Finally, the heat transfer due to radiation among the absorber plate and the bottom plate is extracted from equation (12) [13].

$$h_{r,p-b} = \frac{\sigma (T_p + T_b)(T_p^2 + T_b^2)}{\left(\frac{1}{\varepsilon_p}\right) + \left(\frac{1}{\varepsilon_b}\right) - 1} \quad (12)$$

The heat transfer coefficient due to convective heat transfer between the absorber plate and the glass cover is worked out by carrying out the following calculations.

$$h_{c,p-g} = Nu_{p-g} \left(\frac{k_a}{d_{pg}}\right) \quad (13)$$

Nusselt number is a coefficient which does not have any dimensions. It represents how heat transfer enhances through a fluid layer by fluid motion. Nusselt number, Nu essentially shows us the how convective and conductive heat transfer relate to each other in a fluid layer, and is presented by a ratio. It is defined by equation (14) in heat transfer literature. A greater Nusselt number means there is more effective convection. [14]

$$Nu = \frac{h_c D_h}{k_{Tf}} \tag{14}$$

The Nusselt number is calculated for the absorber plate and the glass cover [14]:

$$Nu_{p-g} = 1 + 1.44\left[1 - \frac{1708}{Ra\,cos\theta}\right]^{+}\left[1 - \frac{1708(\sin 1.8\theta)^{1.6}}{Ra\,cos\theta}\right] + \left\{\left[\frac{Ra\,cos\theta}{5830}\right]^{0.333} - 1\right\}^{+} \tag{15}$$

The superscript + is to ensure that only positive values are used in the brackets that contain it. Otherwise, the bracket should be set equal to zero.

$$h_{c,p-g} = \frac{k_a}{d_{pg}}\left(1 + 1.44\left[1 - \frac{1708}{Ra\,cos\theta}\right]^{+}\left[1 - \frac{1708(\sin 1.8\theta)^{1.6}}{Ra\,cos\theta}\right] + \left\{\left[\frac{Ra\,cos\theta}{5830}\right]^{0.333} - 1\right\}^{+}\right) \tag{16}$$

Next Rayleigh number is calculated. Rayleigh number is a dimensionless number which represents the ratio of forces due to buoyancy in a fluid in comparison to the products of the thermal and momentum diffusivities. [14]

$$Ra = \frac{g\beta' Pr}{\nu^2}\left[T_p - T_g\right]d_{pg}^{\,3} \tag{17}$$

g is the gravitational acceleration due to the force of gravitation, and is taken as 9.81 m/s^2. ν is the kinematic viscosity of air and has the units m^2/s.

$$\nu = \frac{\mu}{\rho_a} \tag{18}$$

β' is the volumetric coefficient of expansion. This is a property which represents how density changes with varying temperature, when pressure is kept as constant. [14]

$$\beta' = \frac{1}{T} \tag{19}$$

The average sum of the glass cover and the absorber plate temperatures are noted as T.

$$T = \frac{T_p + T_g}{2} \tag{20}$$

Prandtl number can be determined using equation (21). Prandtl number is a number with no dimensions. It is used to estimate the relation of molecular diffusivity of momentum to molecular diffusivity of heat. [14]

$$\text{Pr} = \frac{\mu c_p}{k_a} \tag{21}$$

The thermal properties density, ρ_a , heat conductivity coefficient, k_a, dynamic viscosity, μ, and specific heat capacity of air, $c_p$within the temperature range 280K-480K are estimated using the following correlations, respectively. [9]

Density of air, ρ_a (kg/m^3):

$$\rho_a = 3.9147 - 0.016082T_f + 2.9013 \times 10^{-5}T_f^2 - 1.9407 \times 10^{-8} \times T_f^3 \tag{22}$$

Heat conductivity coefficient, k_a (W/mK):

$$k_a = \left(0.0015215 + 0.097459T_f - 3.3322 \times 10^{-5}T_f^2\right) \times 10^{-3} \tag{23}$$

Dynamic viscosity of air, μ (kg/ms):

$$\mu = \left(1.6157 + 0.06523\, T_f - 3.0297 \times 10^{-5}T_f^2\right) \times 10^{-6} \tag{24}$$

Specific heat coefficient of air, c_p (J/kgK):

$$c_p = 999.2 + 0.1434\, T_f + 1.101\ \times 10^{-4}\, T_f^2 - 6.7581 \times 10^{-8}T_f^3 \tag{25}$$

Convection heat transfer also takes among working medium, which is the flowing air, and the absorber plate, and between the working medium and the bottom plate. The convective heat transfer coefficients are denoted as h_1 and h_2, respectively. h_1 and h_2 are of equal values and can be determined in the following manner. [8]

$$h_1 = h_2 = \left(\frac{k_{Tf}}{D_h}\right) Nu \tag{26}$$

The Nusselt number is calculated with different correlations, depending on if the flow could be said to be laminar or turbulent.

When the flow regime can be said to be laminar (Re < 2100) in the rectangular channel, the Nusselt number correlation is [15]:

$$Nu = 4.4 + \frac{0.00398(0.7ReD_h/L_c)^{1.66}}{1+0.0114(0.7ReD_h/L_c)^{1.12}} \quad (27)$$

However, when the flow regime can be said to be fully developed turbulent flow (Re >2300) in the rectangular channel (duct), the correlation for Nu becomes [16]:

$$Nu = 0.0158Re^{0.8} \quad (28)$$

Reynolds number is the proportion of the inertial forces to viscous forces. There will be laminar flow, when viscous forces are in abundance compared to the inertial forces. On the contrary, the flow regime will be turbulent when the inertial forces are larger in proportion to viscous forces. The Reynolds number is determined by equation (29) [14].

$$Re = \frac{\dot{m}D_h}{A\mu} = \frac{\rho_a V_f D_h}{\mu} \quad (29)$$

D_h is the characteristic length equivalent to the duct hydraulic diameter. It is determined differently for the solar air collectors with fins and no fins. [8]

Without fins:

$$D_h = \frac{2(BH)}{B+H} \quad (30)$$

With fins:

$$D_h = \frac{4[BH - L_t W_t N_{ti}]}{2(B+H+L_t N_{ti})} \quad (31)$$

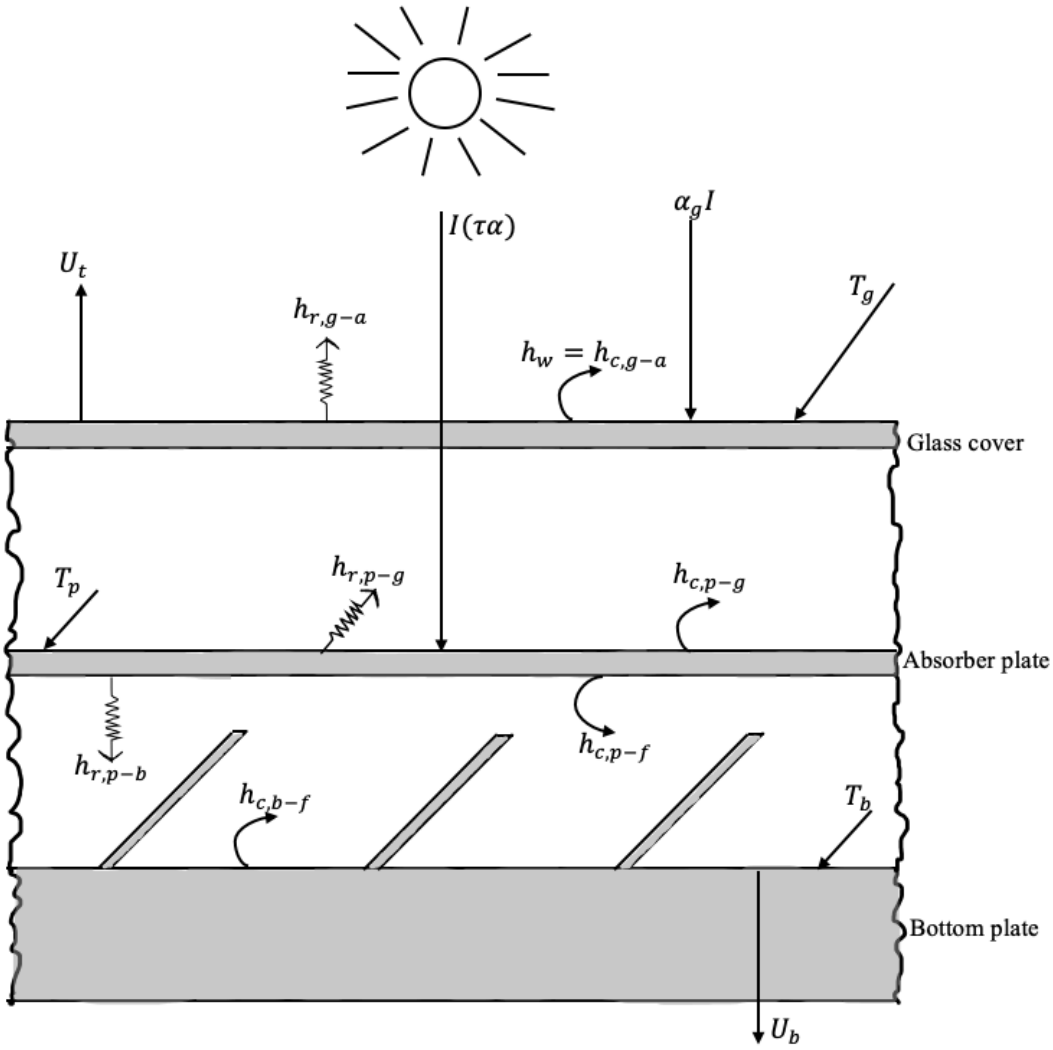

Figure 3: Heat transfer coefficients due to convection and radiation shown on the side section of finned solar air heater [8].

3.2.5 Coefficients of Heat Losses

Heat loss coefficients of the front side, U_t is determined in equation (32). [5]

$$U_t = \left(\frac{N_g}{\frac{C}{T_p}\left[\frac{T_p - T_a}{N_g + f}\right]^{0.33} + \frac{1}{h_w}} \right)^{-1} + \frac{\sigma(T_p - T_a)(T_p^2 - T_a^2)}{\frac{1}{\varepsilon_p + 0.05 N_g (1-\varepsilon_p)} + \frac{2N_g + f - 1}{\varepsilon_p} - 1} \tag{32}$$

N_g is the number of glass covers. Moreover, the correlations C and f are used in the calculation of U_t. [8]

$$C = 365.9[1 - 0.0083\,\theta + 0.0001298\,\theta^2] \tag{33}$$

$$f = (1 - 0.04\,h_w + 0.0005 h_w^2)\left(1 + 0.091 N_g\right) \tag{34}$$

The coefficient of heat loss of the bottom face is computed using equation (35). The bottom side of the solar air collectors are well insulated. Hence, the properties of the insulation material are considered for the U_b calculation. [9]

$$U_b = \frac{k_S}{\delta_S} \tag{35}$$

The total heat loss coefficients, or in other words, the overall heat loss coefficients are calculated using different correlations for the finned and non-finned solar collectors. For the solar air collector without fins, the calculation of the overall heat loss is calculated in a straightforward manner. However, for the finned solar air collector, a non-dimensional quantity, ϕ is introduced when determining of the overall coefficient of heat loss. [8]

Without fins:

$$U_L = U_t + U_b \tag{36}$$

With fins:

$$U_L = \frac{(U_b+U_t)(h_1h_2\phi+h_1h_2+h_2\phi h_r)+U_bU_t(h_1+h_2\phi)}{h_1h_r+h_2\phi U_t+h_2\phi h_1+h_1h_2\phi} \tag{37}$$

ϕ is a dimensionless quantity that is used to measure fin effectiveness. In the solar air collector without fins, this quantity is taken as 1. [6]

Without fins:

$$\phi = 1 \tag{38}$$

With fins:

$$\phi = 1 + \left(\frac{A_f}{A_c}\right)\eta_f \tag{39}$$

The fin efficiency is denoted as η_f and is calculated using equation (40). [13]

$$\eta_f = \left[\frac{\tanh{(ML_t)}}{ML_t}\right] \tag{40}$$

M is a correlation which is used for the fin efficiency calculations.

$$M = \sqrt{2h_c/h_f t_f} \tag{41}$$

3.2.6 Performance of The Solar Air Heaters

The solar air heater efficiency: [8]

$$\eta = \frac{Q_u}{A_c I} \tag{42}$$

The useful heat gain is determined in the following fashion:

$$Q_u = A_c F_R [S - U_L(T_i - T_a)] \tag{43}$$

The absorber plate absorbs solar radiation and this is determined by:

$$S = I(\tau\alpha)_{effective} \tag{44}$$

$\tau\alpha$ is the transmitted absorption coefficient, and the approximation of its value is determined from the relation provided in equation (45).

$$(\tau\alpha)_{effective} \cong 1.01\tau\alpha \tag{45}$$

Heat removal factor is a ratio which represents the relation of how much heat transfer there is actually to maximum attainable heat transfer, and is defined by equation (46). [13]

$$F_{HR} = \frac{\dot{m}c_p}{A_c U_L}\left\{1 - exp\frac{A_c U_L F'}{\dot{m}c_p}\right\} \tag{46}$$

The heat removal factor is different for the solar air collectors with fins and no fins. This is due to the collector efficiency factor, F' is calculated in differently for the former and the latter. F' is determined in the following approach.[8,12]

Without fins:

$$F' = \frac{h}{h + U_L} \tag{47}$$

h is a non-dimensional number which is deduced by:

$$h = h_{c,p-a} + \frac{1}{\left(\frac{1}{h_{c,b-a}}\right) + \left(\frac{1}{h_{r,p-b}}\right)} \tag{48}$$

With fins:

$$F' = \frac{h_r h_1 + h_2 \phi U_t + h_2 \phi h_r + h_r h_1 \phi}{(U_t + h_r + h_1)(U_b + h_2 \phi + h_r) - h_r^2} \tag{49}$$

The corrected outlet air temperature is estimated as [8]:

$$T_0 = T_i + \frac{1}{U_L}[S - U_L(T_i - T_a)\,]\left[1 - \exp\left(-\frac{A_c U_L F'}{\dot{m} c_p}\right)\right] \quad (50)$$

3.3 Solution of The Developed Model

The analytical model developed to calculate the heat transfer coefficients, heat losses, collector efficiencies, and outlet air temperatures is numerically solved in MATLAB-R2020b. The numerical calculation procedure uses an iterative method. In Figure 4 the numerical analysis procedure of the model is presented in a flowchart. The input parameters inserted into the code developed in MATLAB are provided in Table 1.

The iterative numerical method is solved in the following manner:

1. The input parameters of the system and the environment are inserted.
2. Guesses for the initial values of the temperatures of working medium, T_f,glass cover,T_g, absorber plate ,T_p and bottom plate, T_b are made.
3. The properties of air are estimated.
4. The coefficients of heat transfer are computed.
5. The new values of the temperatures T_f,T_g ,T_p,T_b are computes using the guessed temperature values.
6. The difference between the newly computed and the initially guessed values of the temperatures is calculated. If the calculated difference is less than or equal to 0.001, then the guessed temperature values are considered to be valid. If not, then the procedure is repeated until the guessed temperature values are satisfactory.
7. Once the iteration procedure is completed, the system performance calculations are carried out.

Table 1: Input parameters inserted into the numerical simulation developed in MATLAB-R2020b.

Input Parameter		**Value**
Surface area of collector	A_c (m^2)	1
Collector length	L_c (m)	1.25
Air channel width	B (m)	0.8
Air channel depth	H (m)	0.04
Total surface area of fins	A_f (m^2)	0.18
Height of fins	L_t (m)	0.05
Width of fins	W_t (m)	0.035
Thickness of fins	t_f (m)	0.0007
Number of fins per row	N_{ti}	8
Number of fins attached	N_t	80
Thickness of insulator	δ_s (m)	0.05
Distance between absorber plate and glass cover	d_{pg} (m)	0.03
Number of glass covers	N_g	1
Tilt angle of the collector	θ	31
Thermal conductivity of fins	k_t (W/mK)	48
Thermal conductivity of insulator	k_s (W/mK)	0.045
Emissivity of glass cover	ε_g	0.88
Emissivity of absorber plate	ε_p	0.9
Emissivity of bottom plate	ε_b	0.9
Stefan- Boltzmann constant	σ (W/m^{2}K^4)	5.67×10^{-8}
Absorptivity of absorber plate	α	0.9
Transmissivity of glass cover	τ	0.92
Flowing air velocity	V_f (m/s)	2.5

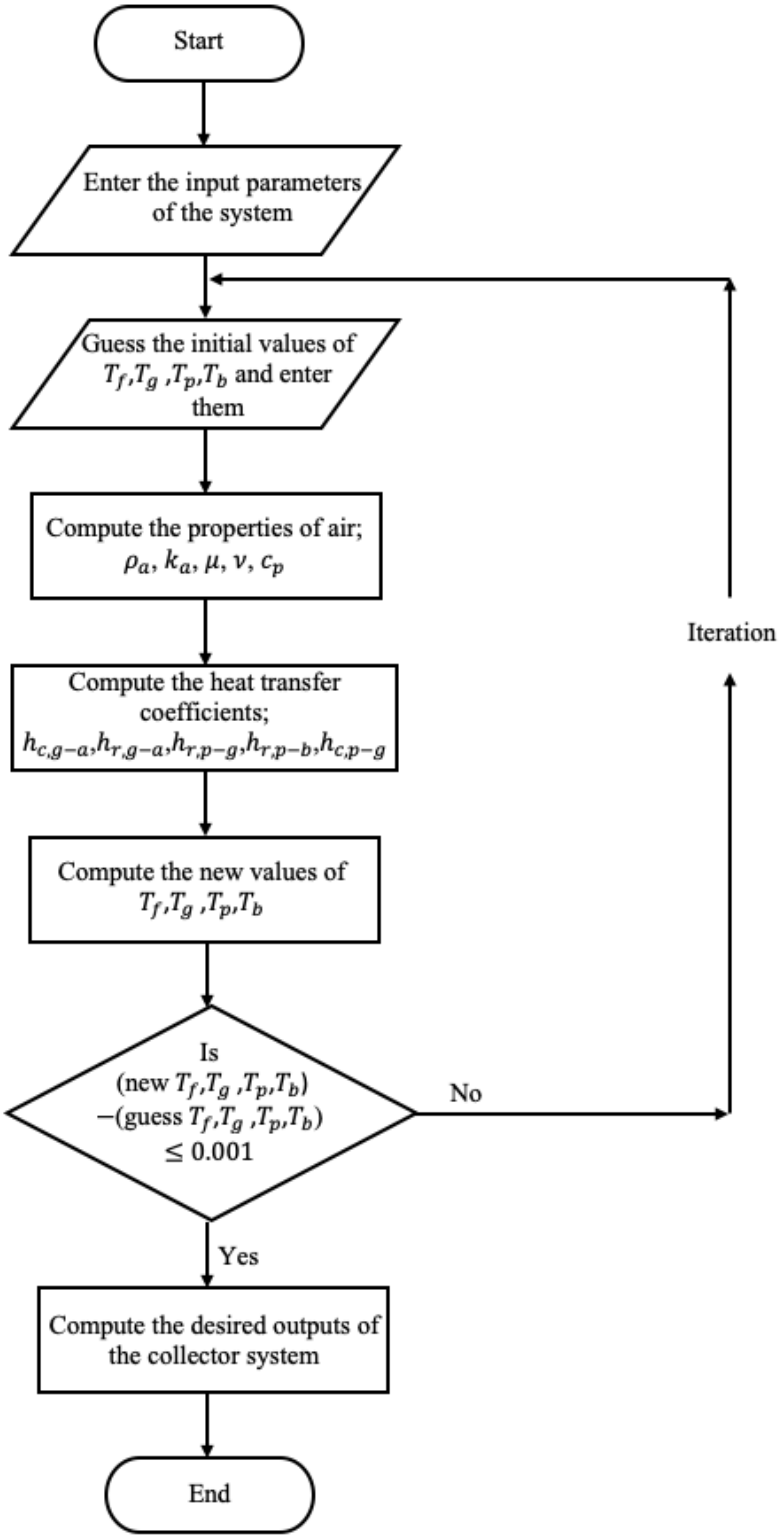

Figure 4: Flowchart demonstrating the numerical procedure carried out on MATLAB-R2020.

Chapter 4

RESULTS AND DISCUSSIONS

This segment covers the results obtained for the performance of the solar air heater with and without fins with respect to varying air mass flow rates ranging from 0.01 to 0.09 kg/s and solar irradiance ranging from 300 to 1200 W/m^2. The impact of fins on the heater performance was examined by comparing the results obtained for the flat plate solar air collector with fins to the conventional flat plate solar air collector without fins. Furthermore, the outcomes of the present study were compared to the investigations mentioned in the literature review, carried out by Rai et al [13] and Kumar and Chand [10].

4.1 Heat Losses

The installation of rectangular fins to the bottom plate resulted in a decrease in the total heat loss coefficients. The overall heat loss coefficient of the solar air heater without fins was determined to be 3.75 W/m^{2}K. It has been observed that the addition of fins to the system reduced the overall heat loss value to 3.58 W/m^{2}K. Reduction in overall heat loss coefficients is desirable in solar air collectors as it leads to an increase in the useful energy gain, as equation (43) suggests. This, in turn, aids in the improvement of collector efficiencies. It should also be noted that the heat loss coefficients from the front and the bottom side of the collector are 2.85 W/m^{2}K and 0.9 W/m^{2}K, respectively. As it can be understood from the values obtained, the there is more heat loss from the front side than there is from the bottom side. This is due to

the fact that insulation precautions were taken for the collector's back side, whilst the front side is in direct contact with the ambience.

4.2 Heat Removal Factor

The solar irradiance value may vary depending on the geographical location, the season of the year, and other factors such as whether it is a clear or a cloudy day. A solar irradiance of 1000 W/m^2 is an appropriate value to use for the evaluation of solar air heaters, considering that is a common average value obtained in experimental studies, and is widely used in numerical investigations.

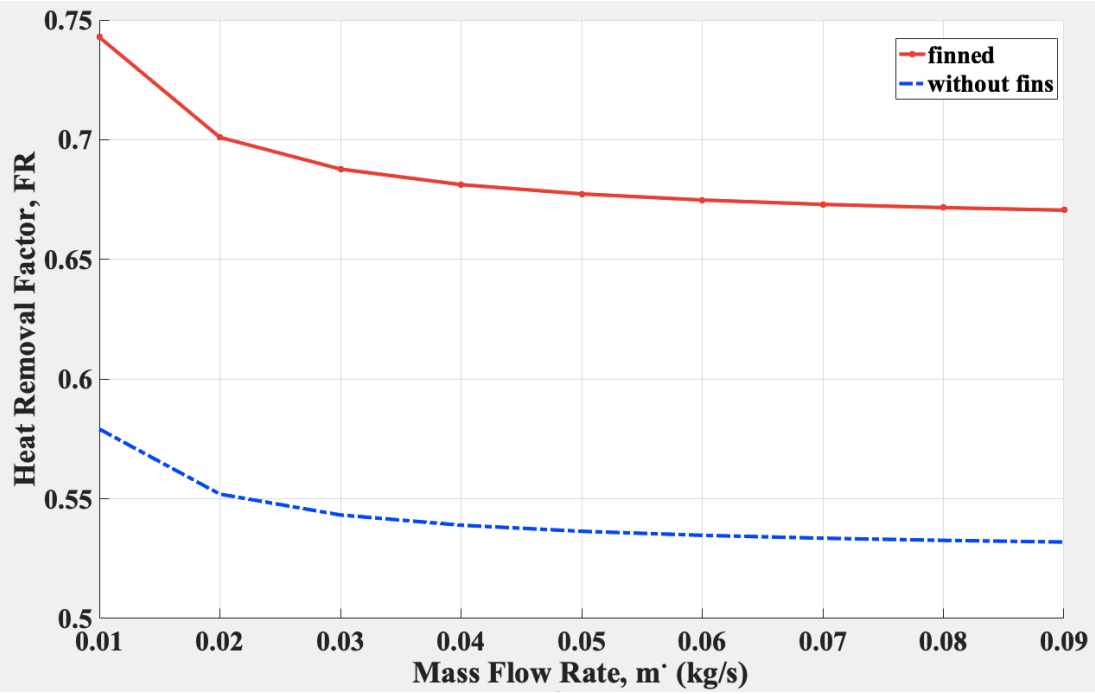

Figure 5: Heat removal factor with varying mass flow rates, at I = 1000 W/m^2.

By fixing the solar insolation (irradiance) value to 1000 W/m^2, the heat removal factor was computed for a variety of air mass flow rates in the range 0.01-0.09 kg/s. From the graph in Figure 5, it is observed that the heat removal factor values for the finned solar air heater are greater than the ones of the solar air heater without fins. By definition, this indicates that more actual heat transfer occurs in the finned solar air

heater compared to the solar air heater without fins. This is because the addition of fins leads to an increase in the surface area of the collector, where more heat transfer can take place. Moreover, it is observed that the maximal values of the heat removal factor are secured at a mass flow of 0.01 kg/s for the solar air collectors with fins and without fins, with the values being 0.7428 and 0.5792, respectively. These values drop down to 0.701 and 0.55 at mass flow rate 0.02 kg/s for the finned and conventional solar air heaters, respectively. Then, the heat removal factors continue to decrease steadily with increasing mass flow rates. This indicates that more actual heat transfer occurs at lower mass flow rates for both finned and conventional solar air heaters. Although the heat removal factor values drop as the mass flow rate values get raised, the trend of higher heat removal factors for the finned solar air collectors in comparison with the conventional solar air heater still remains. Higher heat removal factor values lead to increased useful energy gains as equation (43) suggests. Hence, it also leads to increased collector efficiencies as suggested by equation (42).

4.3 Useful Energy Gain with Changing Mass Flow Rate

Again, by fixing the insolation value to 1000 W/m^2, useful energy gain was computed for a variety of air mass flow rates ranging from 0.01-0.09 kg/s.

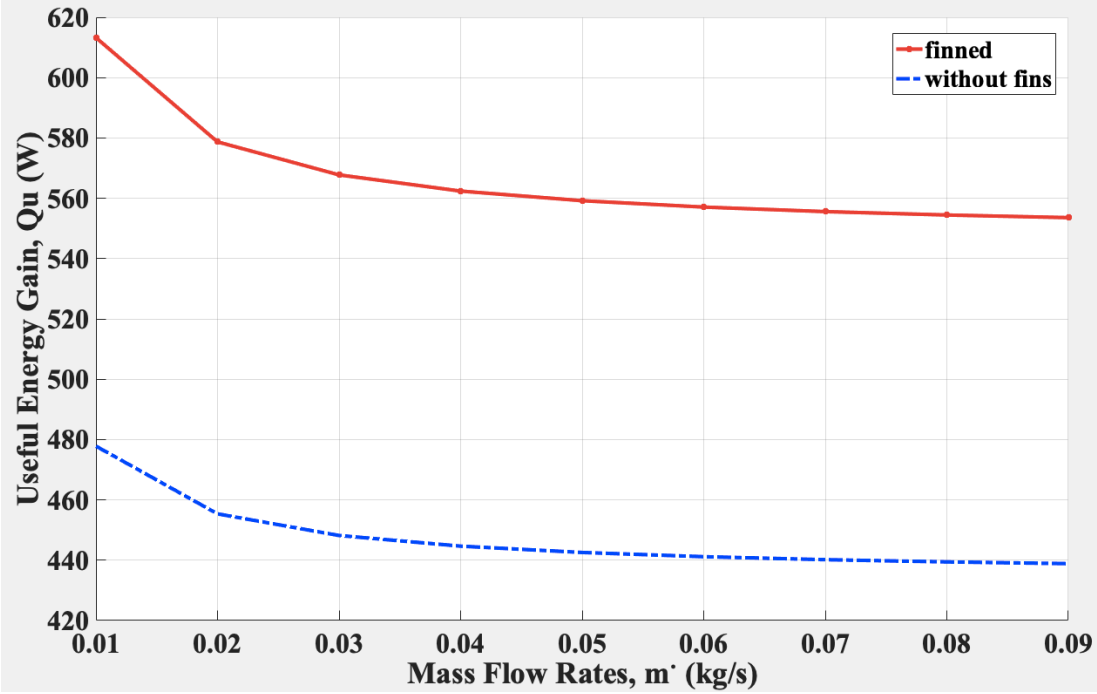

Figure 6: Useful energy gain with varying mass flow rate, I = 1000 W/m^2.

It is observed from the graph in Figure 6 that the finned solar air collectors gain significantly more useful energy than the solar air heaters without fins. The surface area of the collector increases with the addition of fins, and this aids in the rise of useful energy gain, as more heat transfer can take place. A maximum value for the useful energy gain was obtained to be 613.24 W for the finned solar air heater and 477.81 W for collector without fins, at the mass flow rate of 0.01 kg/s. The useful energy gain values drop down to 578.70 W/m^2 and 455.36 W/m^2 for the solar air heaters with and without fins, respectively, at that moment that the mass flow rate is changed from 0.01 kg/s to 0.02 kg/s. The useful energy gain continues to decrease steadily for mass flow rates beyond 0.02 kg/s. This indicates that the fins have the

largest impact at reduced mass flow rates, and that the fins do not show a remarkable differences across the mass flow rate ranges 0.03-0.09 kg/s. This could be due to the dimensions and the arrangements of the solar air heater components, as well as the materials used. These are the factors that contribute to the surface conductance. Nevertheless, the values of the useful energy gain for the finned solar air heater remain to be significantly greater than for the solar air heater that does not have any assigned fins, at all air mass flow rates tested.

4.4 Collector Efficiency with Changing Mass Flow Rate

The collector efficiency was calculated for a variety of mass flow rates ranging from 0.01-0.09 kg/s, by keeping the solar irradiance at a constant with the value of 1000 W/m^2. Figure 7 illustrates the variance of the collector efficiencies according to mass flow rates for the finned and conventional solar collectors.

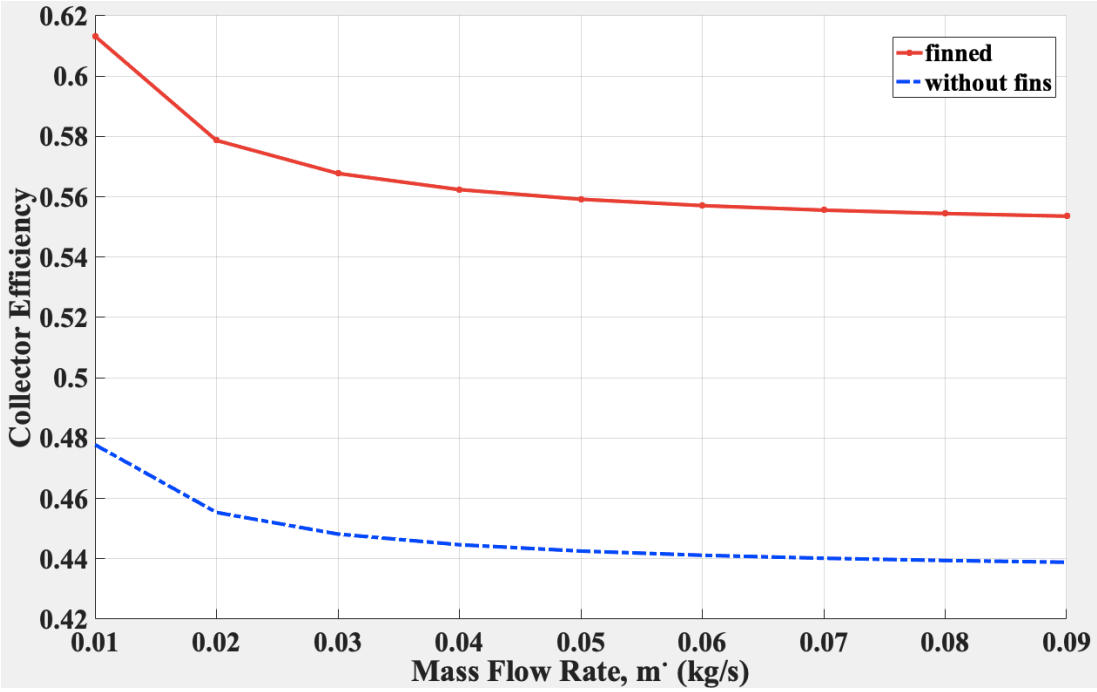

Figure 7: Collector efficiency with varying mass flow rate, I = 1000 W/m^2

The finned collector reaches a maximum collector efficiency of 61.32%, whereas the collector without fins can only reach a maximum collector efficiency of 47.78%, at the mass flow rate 0.01 kg/s. This indicates that adding fins into the design configurations of a solar air heater maximizes the collector efficiency drastically. The efficiency values of the collector start to reduce for mass flow rates beyond 0.01 kg/s. The drop in the efficiency values for both solar air heaters is steeper at the moment that the mass flow rate is boosted from 0.01kg/s to 0.02 kg/s, and past 0.02 kg/s the efficiency values of both collectors continue to decrease in a steadier fashion. At the point where the mass flow rate is 0.09 kg/s, which is the point where minimum efficiencies were achieved, the collector efficiency of the finned solar air collector is 55.36%, whilst it is 43.89% for the conventional solar air heater. Considering that conventional solar air heaters are infamous for their low efficiency values (around 40%), the finned solar air heaters performed very well by raising the efficiency value from 43.89% to 55.36%. The graph in Figure 7 follows the similar trend of the graph in Figure 6, since the collector efficiency is directly related to the useful energy gain.

Once more, it could be stated that the collector efficiencies for the finned solar air heater remain to be significantly greater than for the solar air heater without fins across the whole range of mass flow rates. This is because the fins ensure increased surface area for the heat transfer and allow a better mixing of the fluid, which then raises the heat transfer rates. However, it should also be stated that the maximized performance was only achieved at lower mass flow rates, and beyond mass flow rate 0.03 kg/s, the collector efficiency values approximately stayed the same, with very slight differences. Therefore, it could be understood that the fins have the greatest impact on the collector efficiency at lower air mass flow rates.

4.5 Temperature Rise of Air with Varying Mass Flow Rates

The outlet air temperature exiting the solar air heaters was calculated for the mass flow rate span 0.01-0.09 kg/s, by setting the solar irradiance value to 1000 W/m^2. Further, the initially guessed inlet temperature value was then subtracted from the computed outlet air temperature values. After careful evaluation of literature review and the execution of the iterative procedure, the inlet temperature of the flowing air was taken as, T_i = 303 K. Figure 8 visually demonstrates the impact of fins on the temperature rise of exiting air, and Table 2 provides information about the temperature values obtained for the outlet air.

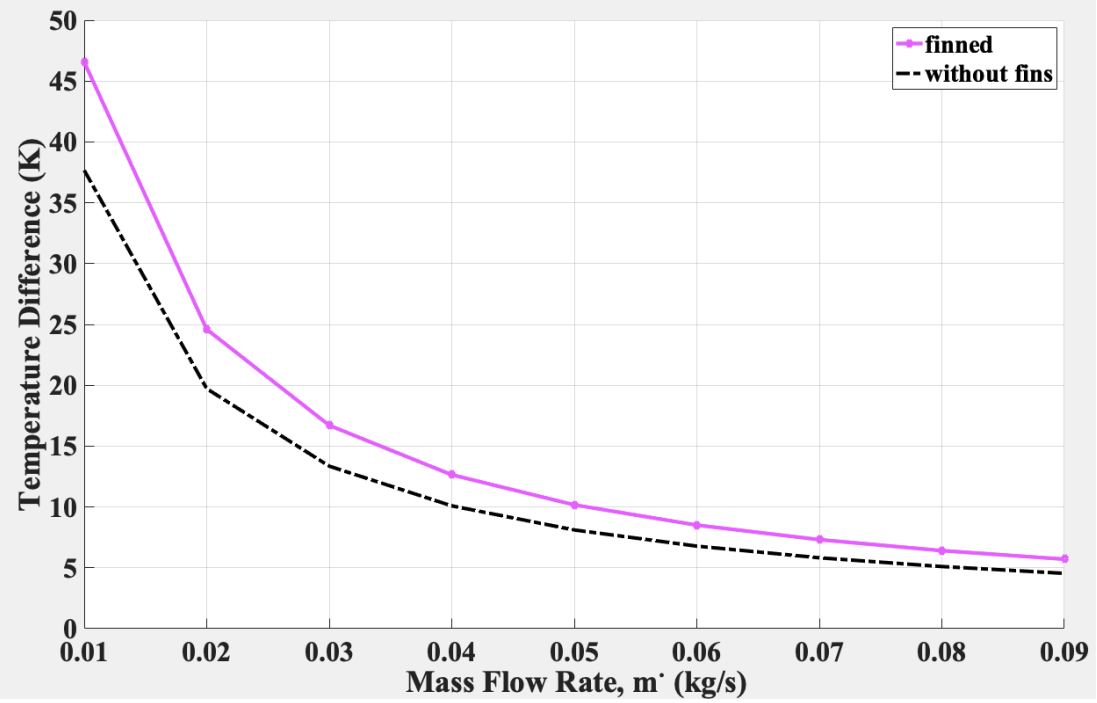

Figure 8: Temperature rise among outlet and inlet air with varying mass flow rates, at I = 1000 W/m^2.

Table 2: Temperature difference between outlet and inlet air with varying mass flow rates, at I = 1000 W/m^2, for the solar air heaters with and with no fins.

$\dot{m}$ (kg/s)	T_O (K) finned	T_O (K) without fins	ΔT (K) finned	ΔT (K) without fins
0.01	349.57	340.67	46.57	37.67
0.02	327.60	322.72	24.60	19.72
0.03	319.70	316.35	16.70	13.35
0.04	315.65	313.09	12.65	10.09
0.05	313.17	311.11	10.17	8.11
0.06	311.51	309.78	8.51	6.78
0.07	310.31	308.83	7.31	5.83
0.08	309.41	308.11	6.41	5.11
0.09	308.71	307.54	5.71	4.54

From Figure 8, it can be observed that the finned solar air heater results in a greater temperature rise of the flowing air compared to the standard solar air heater with no fins. The most considerable difference in the temperature rise of the solar air heaters with fins and without fins is noticed at the mass flow rate 0.01 kg/s. The finned solar air heater causes the temperature of the working medium (flowing air) to rise by 46.57 K, whilst the standard solar air heater makes the temperature rise by 37.67 K. The values of the temperature rise drop drastically when the mass flow rate is changed to 0.02 kg/s. For the finned solar air heater the temperature rise value becomes 24.60 K at 0.02 kg/s, which is significantly lower than the temperature rise obtained at 0.01 kg/s. The graph has an exponential-like trend, where the temperature rise continues to decrease almost exponentially with increasing mass flow rates. Further, the climb of temperature is only 5.71 K for the finned solar air heater at mass flow rate 0.09 kg/s, which is only 1.17 K higher than that of the conventional solar air heater. Therefore, it could be understood that for higher mass flow rates, the enhancement in the temperature rise of exiting air caused by the fins is not as strong. However, these results

are not surprising as it was observed from Figure 6 and 7 that the solar air heaters gained more energy and achieved higher efficiencies at lower mass flow rates. More gained energy results in more heating of the exiting air.

4.6 Useful Energy Gain with Varying Solar Irradiance

Figures 9, 10, 11, 12, 13, 14, 15, 16 and 17 demonstrate the useful energy gain with various values solar irradiance, ranging from 300 W/m^2 to 1200 W/m^2, by fixing the mass flow rate at 0.01, 0.02, 0.03, 0.04 0.05, 0.06, 0.07, 0.08 and 0.09 kg/s, respectively.

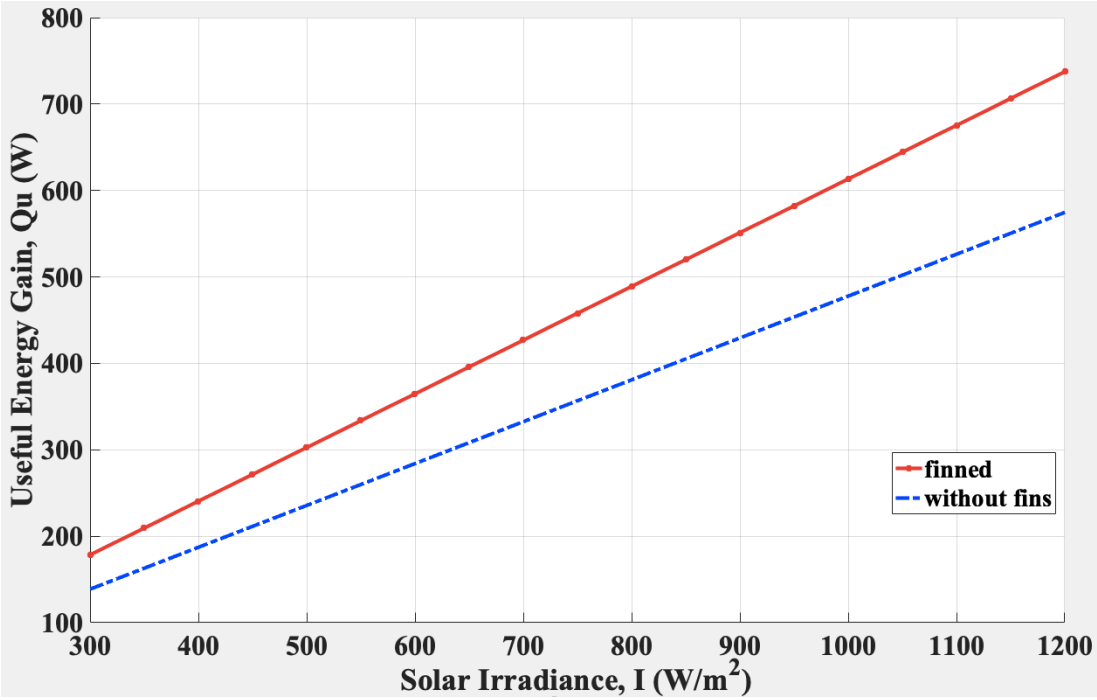

Figure 9: Useful energy obtained with regard to varying solar insolation, $\dot{m}$ =0.01 kg/s

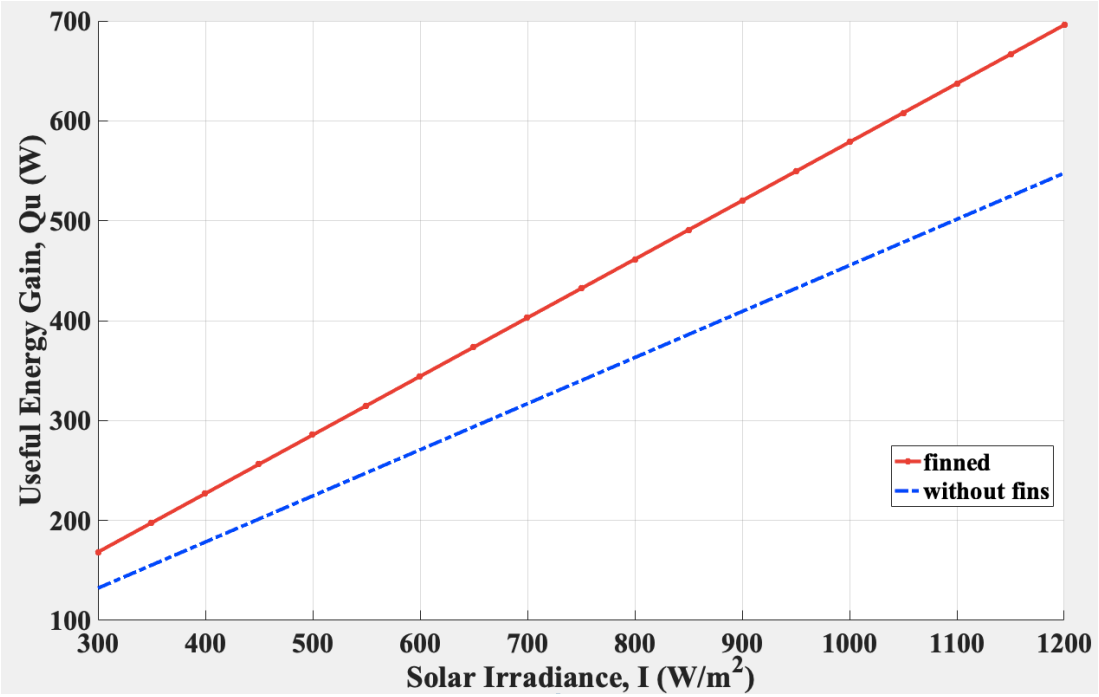

Figure 10: Useful energy obtained with regard to varying solar insolation, $\dot{m}$ =0.02 kg/s

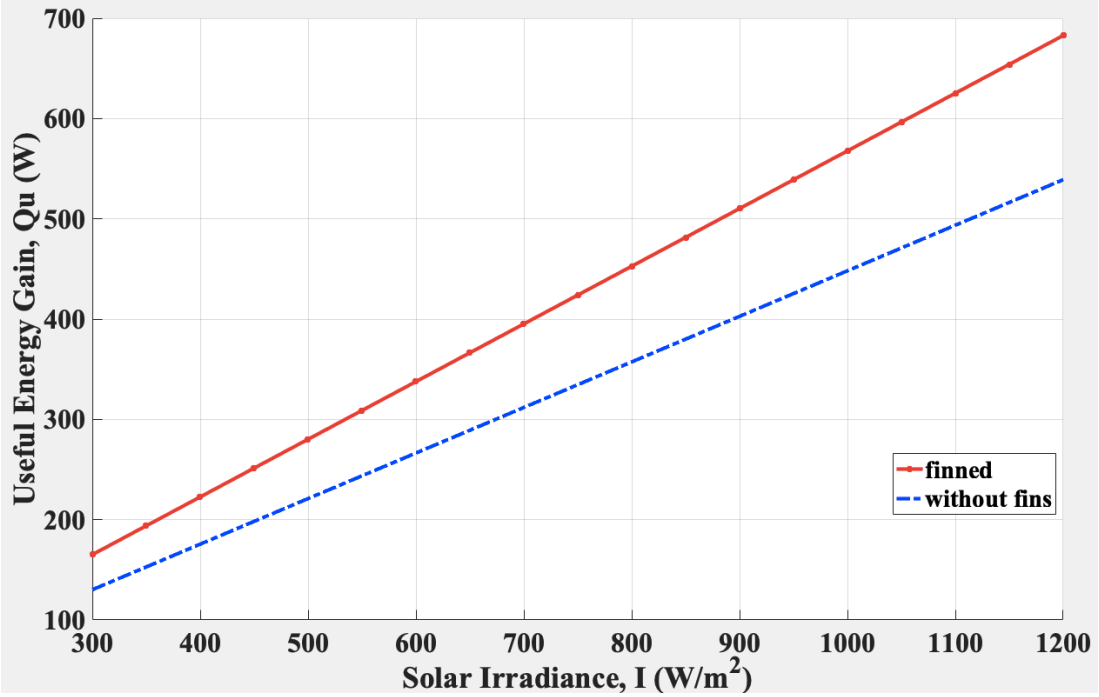

Figure 11: Useful energy obtained with regard to varying solar insolation, $\dot{m}$ =0.03 kg/s

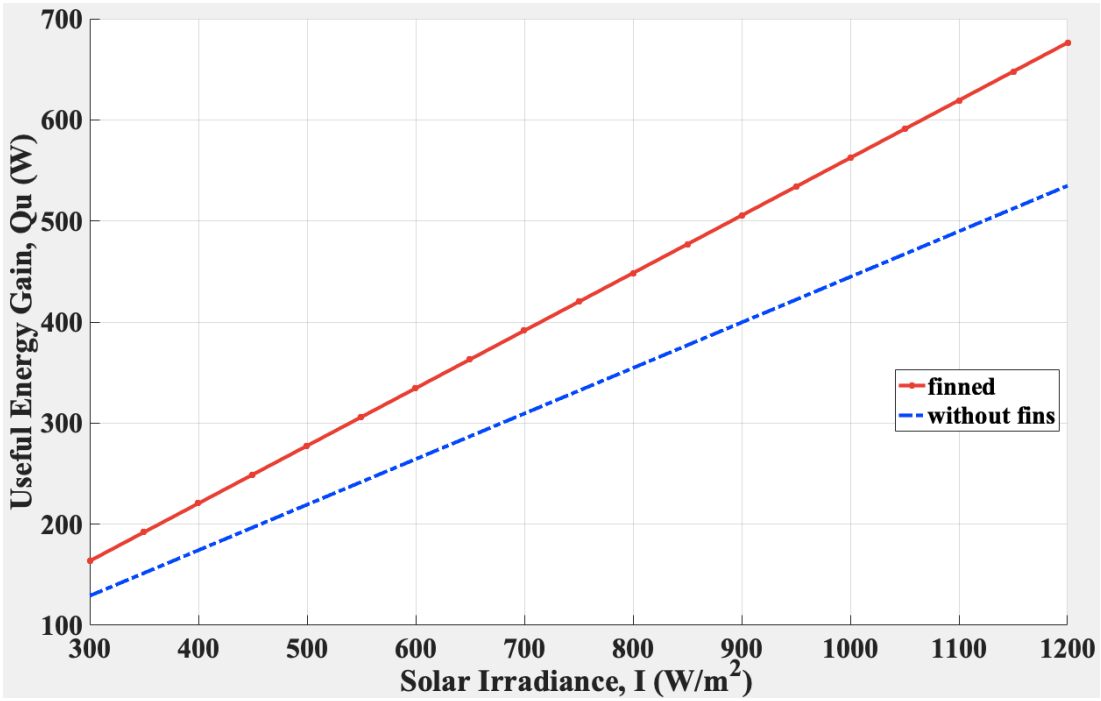

Figure 12: Useful energy obtained with regard to varying solar insolation, $\dot{m}$ =0.04 kg/s

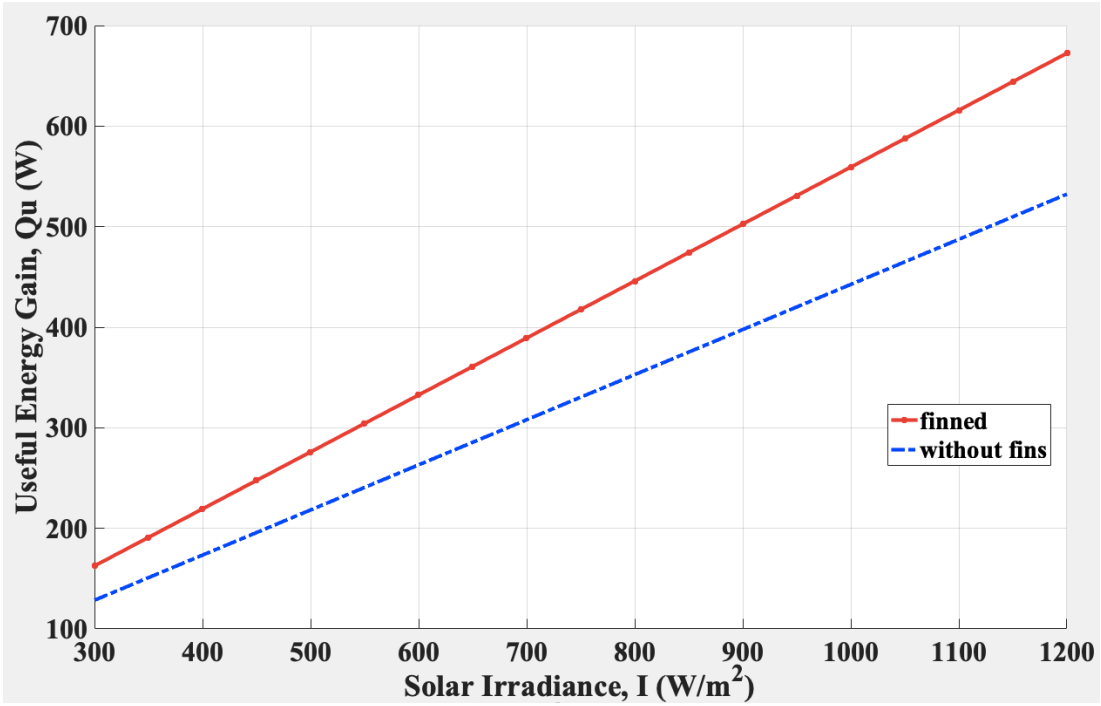

Figure 13: Useful energy obtained with regard to varying solar insolation, $\dot{m}$ =0.05 kg/s

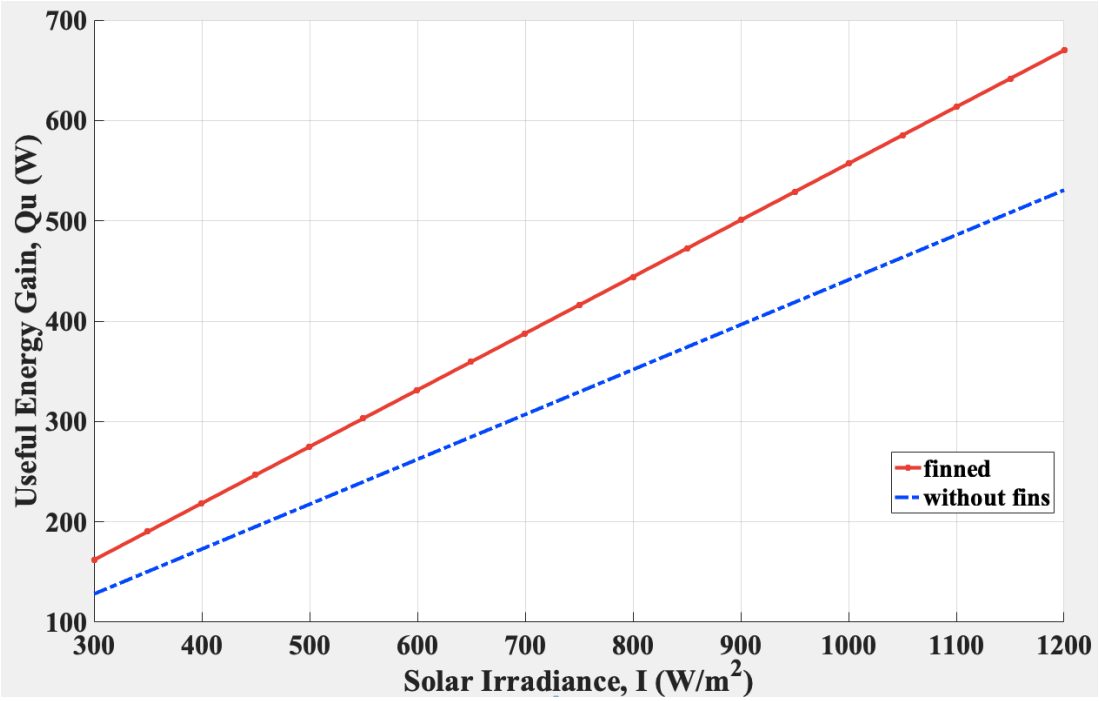

Figure 14: Useful energy obtained with regard to varying solar insolation, $\dot{m}$ =0.06 kg/s

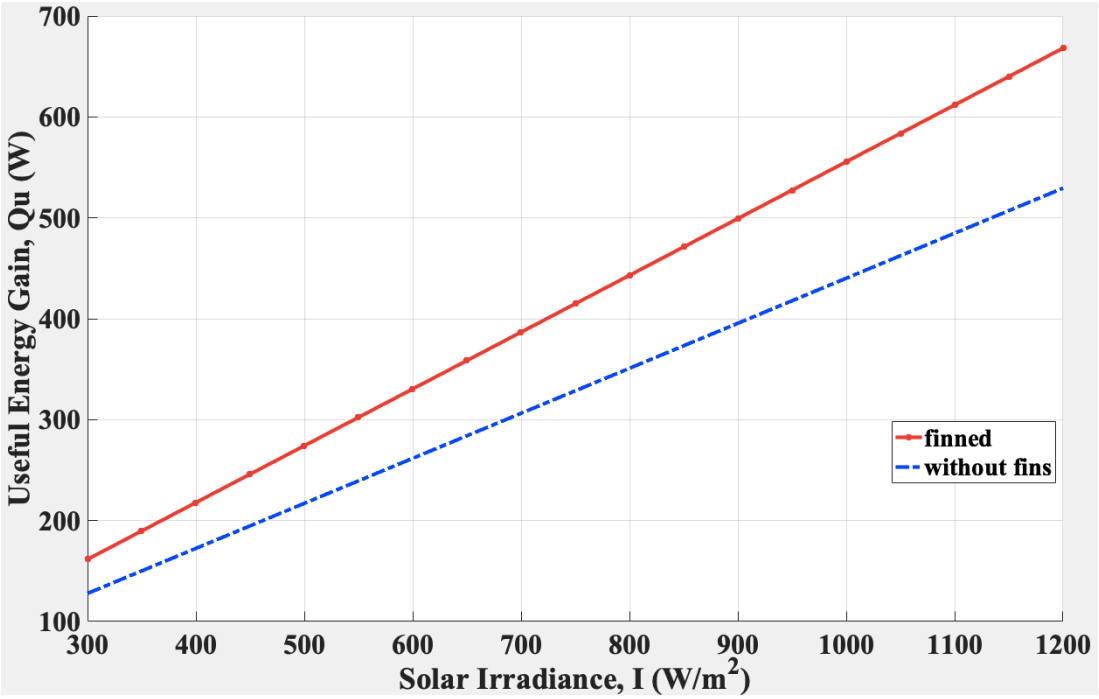

Figure 15: Useful energy obtained with regard to varying solar insolation, $\dot{m}$ =0.07 kg/s

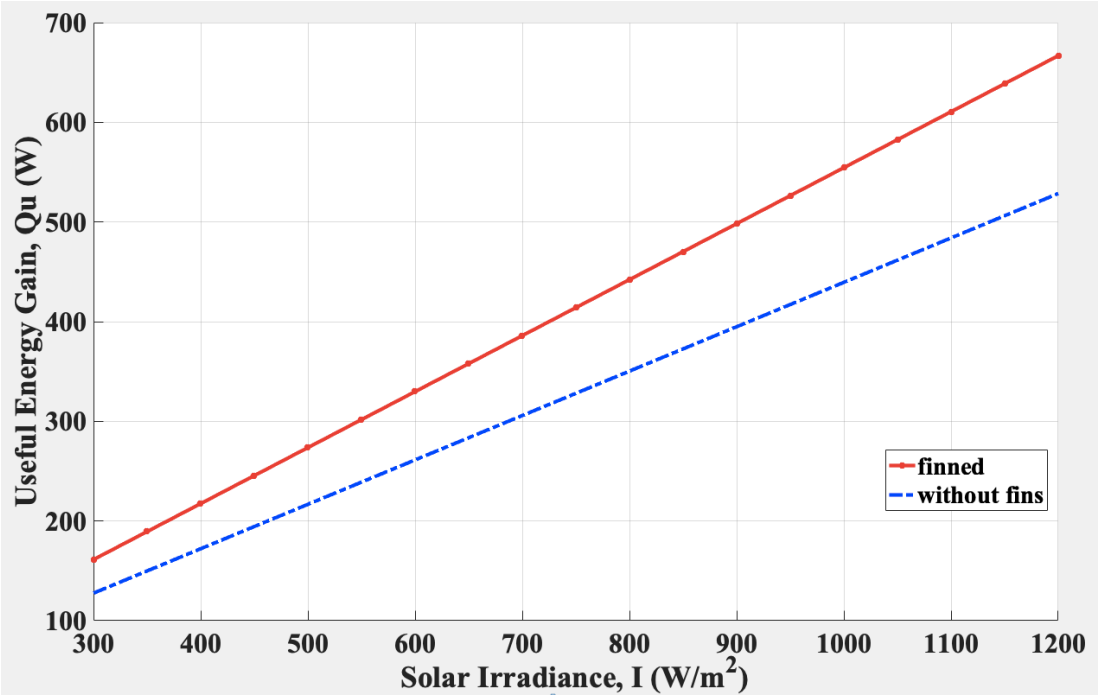

Figure 16: Useful energy gain with regard to varying solar insolation, $\dot{m}$ =0.08 kg/s

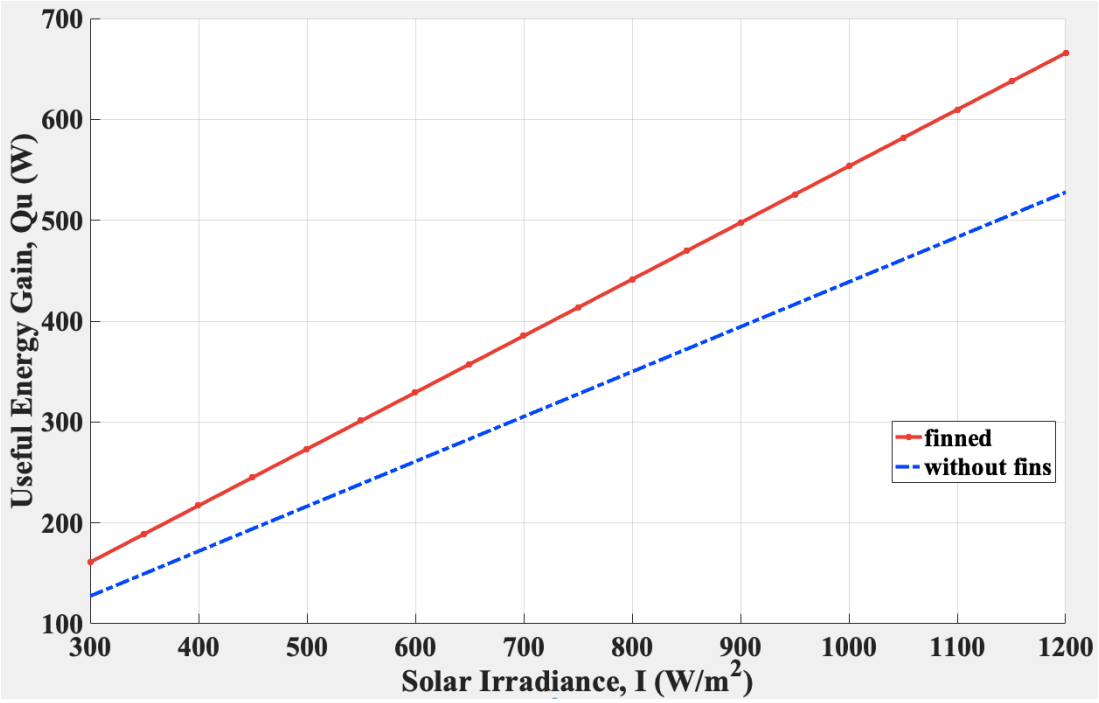

Figure 17: Useful energy obtained with regard to varying solar insolation, $\dot{m}$ =0.09 kg/s

The graphs have the general trend of increased useful energy gain with increased solar irradiance. The useful energy gain is maximized for both of the solar air heaters when the solar irradiance reaches 1200 W/m^2, for all ranges of fixed mass flow rates. However, this is expected, because a higher solar irradiance value means there is more solar energy for the solar air heater to utilize per unit area. The highest useful energy gain values were achieved at the mass flow rate 0.01 kg/s. It is observed that beyond mass flow rate 0.01 kg/s, the performance of the solar air heaters in terms of useful energy gain starts to drop steadily. Even so, it is perceived that the finned solar air heater obtained higher useful energy values in comparison to conventional solar air heater across the range of mass flow rates.

Out of all the combinations of solar irradiance and mass flow rate values computed and tested, the maximum useful energy gain obtained for the solar air heaters is achieved at a solar irradiance of 1200 W/m^2 and a fixed mass flow rate of 0.01 kg/s. Moreover, the highest useful energy gained, at 1200 W/m^2 and 0.01 kg/s, by the finned solar air collector is 737.49 W, whereas it is 574.68 W for the solar air collector without fins. The difference between the useful energy gains of the solar air collectors grows massively with increased solar irradiance levels. It could be examined from Figure 9 that the finned solar air heaters gain only 39.61 W more useful energy than the solar air heaters without fins at a solar irradiance of 300 W/m^2. That being said, the finned solar air heaters gain 162.81 W more useful energy than the solar air heaters without fins at a solar radiance of 1200 W/m^2. In other words, by increasing solar irradiance, the impact of the fins on the collector performance gets more significant.

4.7 Collector Efficiency with Varying Solar Irradiance

Figures 18, 19, 20, 21, 22 23, 24, 25 and 26 demonstrate the collector efficiency values of the finned and non-finned air collectors with solar irradiance values ranging from 300 W/m^2 to 1200 W/m^2, while the mass flow rate is kept at a constant of 0.01, 0.02, 0.03, 0.04, 0.05, 0.06, 0.07, 0.08 and 0.09 kg/s, respectively.

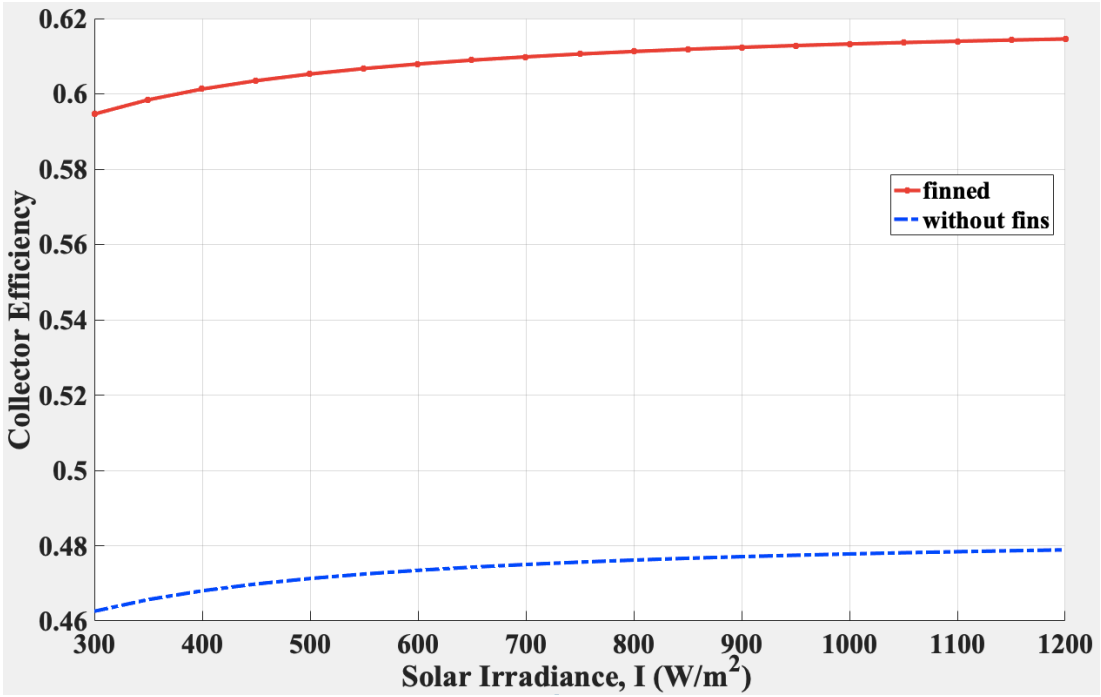

Figure 18: Collector efficiency with varying solar irradiance, $\dot{m}$ =0.01 kg/s

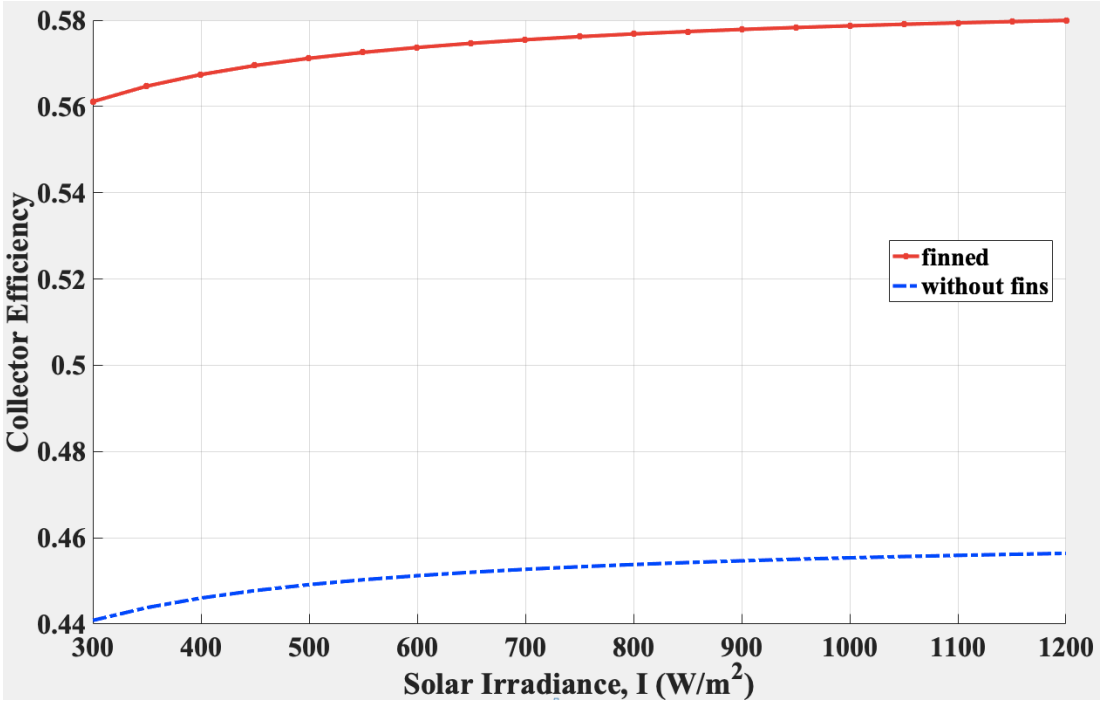

Figure 19: Collector efficiency with varying solar irradiance, $\dot{m}$ =0.02 kg/s

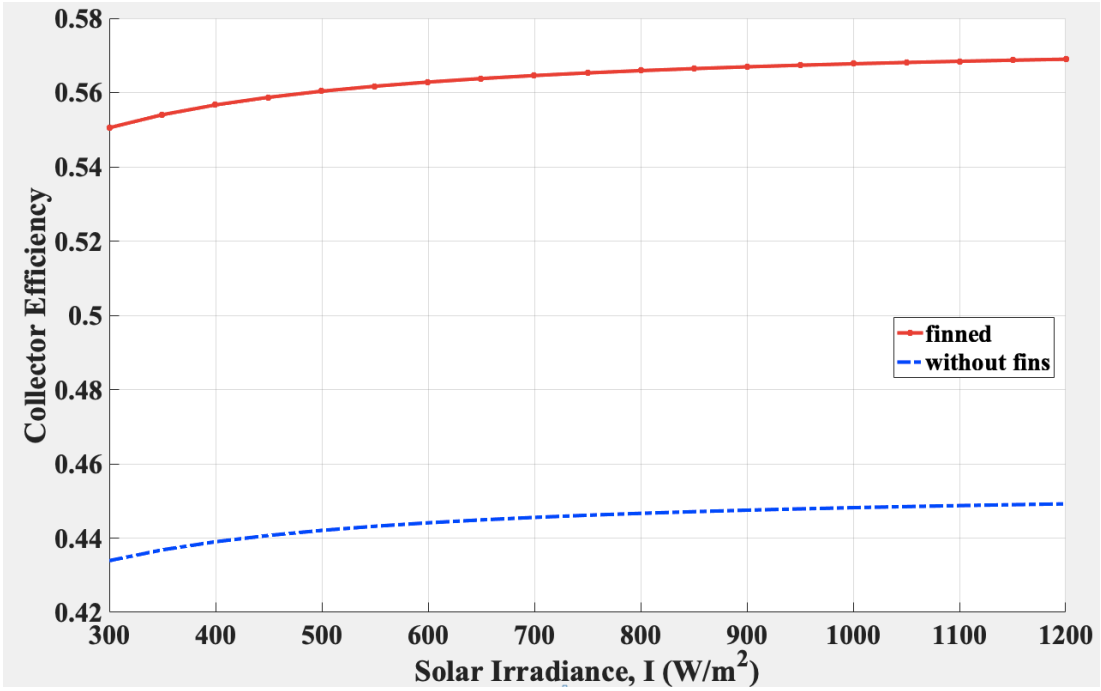

Figure 20: Collector efficiency with varying solar irradiance, $\dot{m}$ =0.03 kg/s

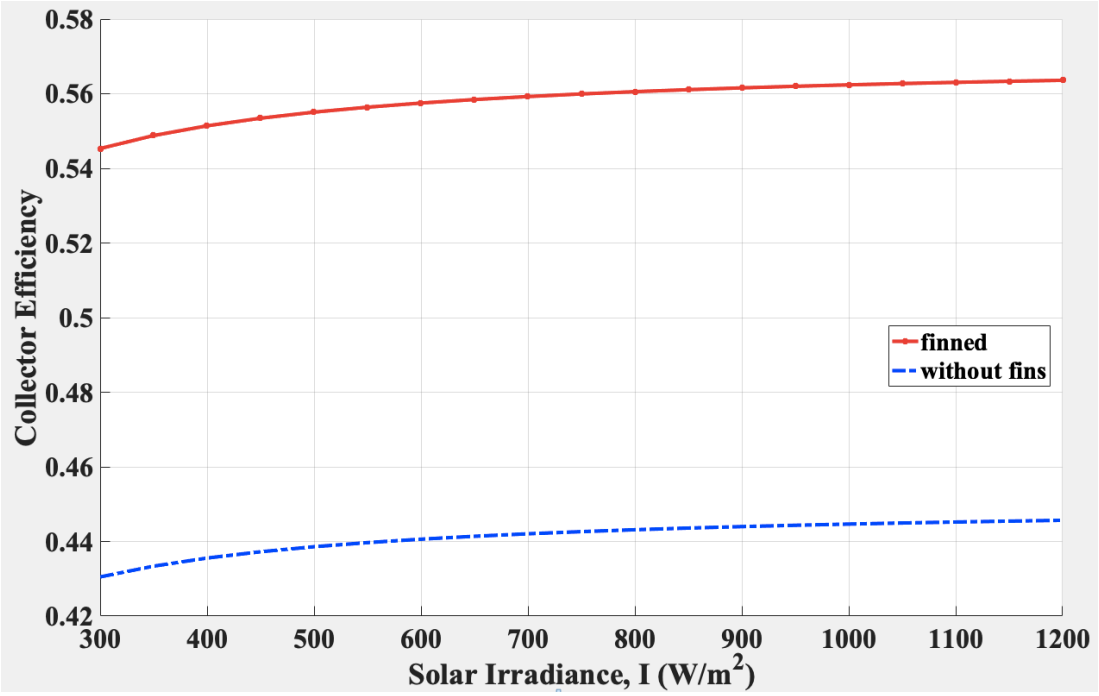

Figure 21: Collector efficiency with varying solar irradiance, $\dot{m}$ =0.04 kg/s

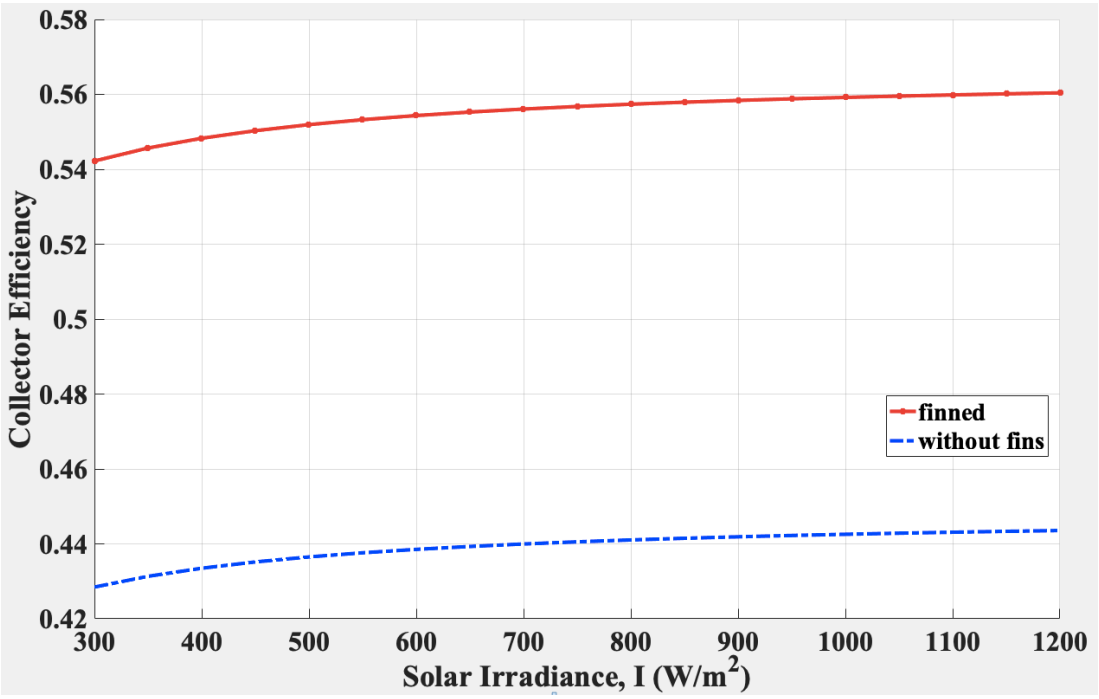

Figure 22: Collector efficiency with varying solar irradiance, $\dot{m}$ =0.05 kg/s

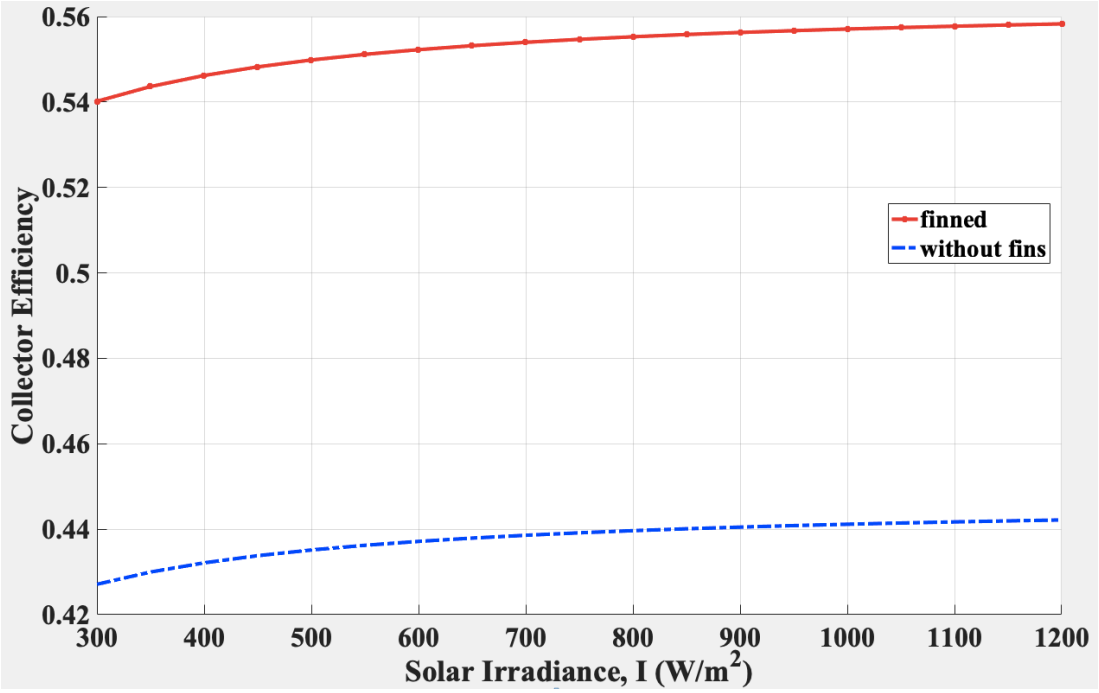

Figure 23: Collector efficiency with varying solar irradiance, $\dot{m}$ =0.06 kg/s

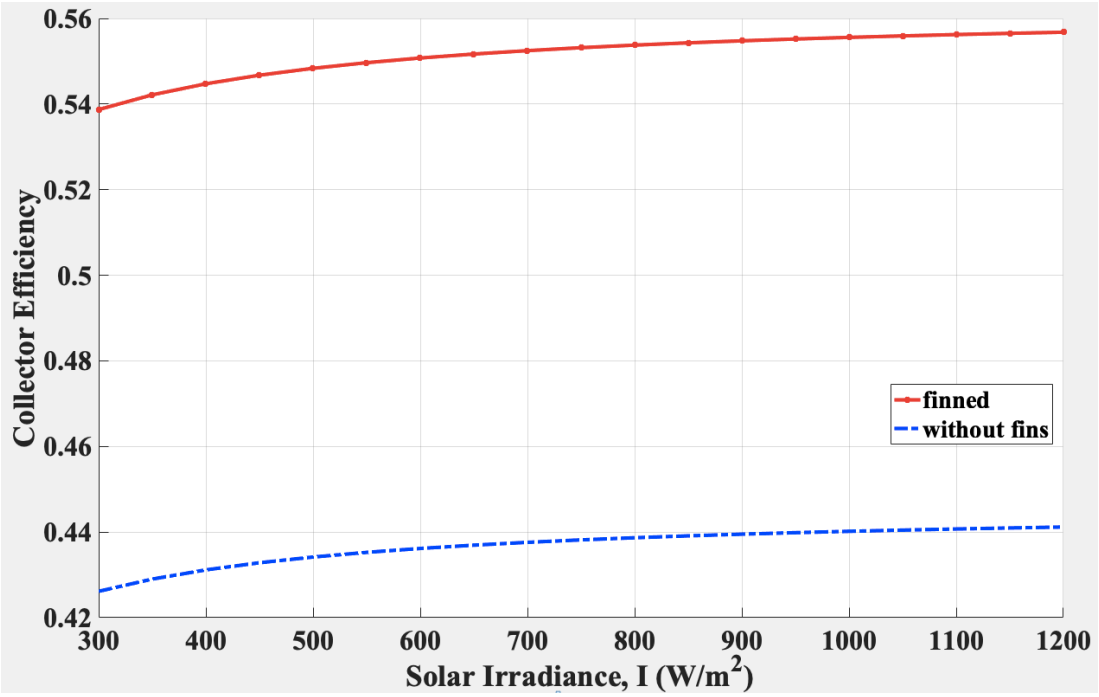

Figure 24: Collector efficiency with varying solar irradiance, $\dot{m}$ =0.07 kg/s

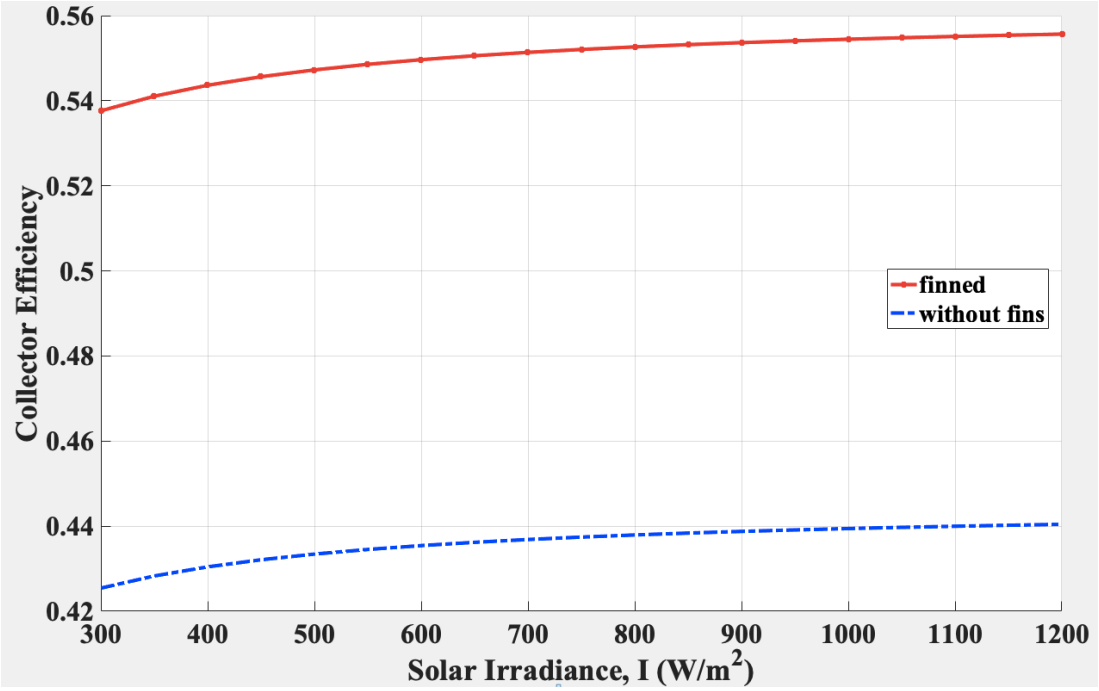

Figure 25: Collector efficiency with varying solar irradiance, $\dot{m}$ =0.08 kg/s

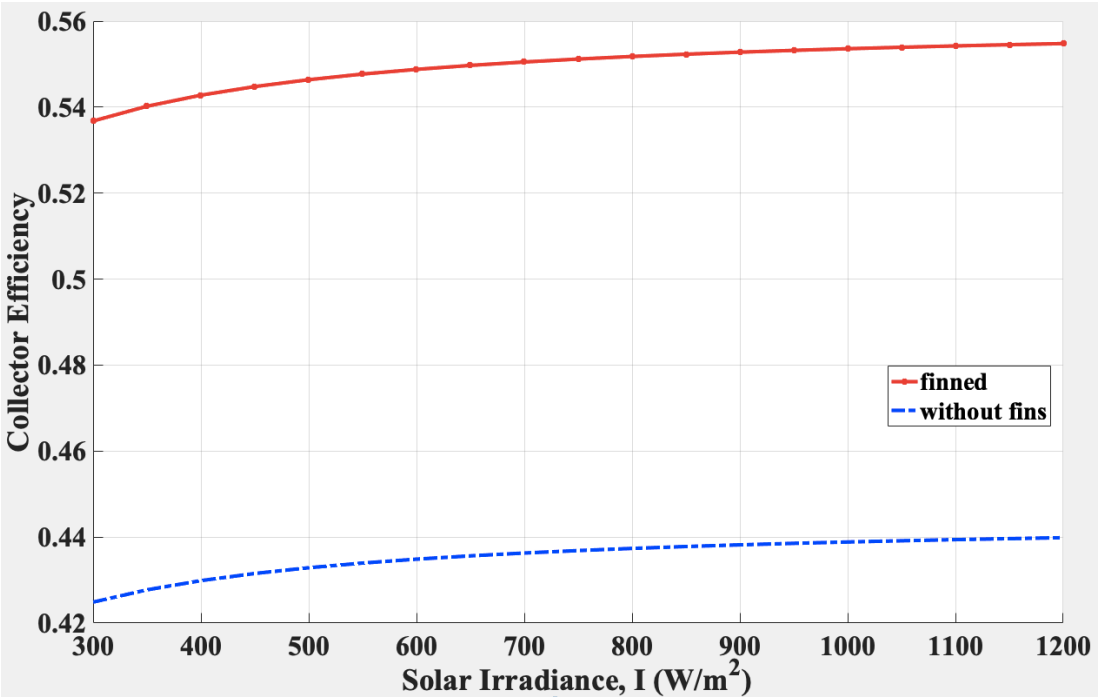

Figure 26: Collector efficiency with varying solar irradiance, $\dot{m}$ =0.09 kg/s

The general pattern of the graphs shows that the assigned fins result in enhanced collector efficiencies. In accordance with the useful energy gain values shown previously, the maximum collector efficiencies were obtained at the mass flow rate of 0.01 kg/s. Further, it is deduced from Figure 18 that a maximum collector efficiency of 61.46% is achieved for the finned solar air collector, whilst the maximum attainable collector efficiency is 47.89% for the solar air collector without fins, at a solar irradiance of 1200 W/m^2 and mass flow rate of 0.01 kg/s. Figure 18 also demonstrates that mass flow rate is 0.01 kg/s, the minimum collector efficiency values are calculated as 59.46% and 46.29% for the finned and non-finned collectors, respectively, when solar irradiance is 300 W/m^2.

Moreover, it seen that across all the mass flow rates tested, the lowest collector efficiency values were obtained at the point where the mass flow rate is fixed to 0.09 kg/s and the solar irradiance is 300 W/m^2. Figure 26 shows that the minimum collector efficiency values at that given point is 53.68% and 42.48% for the solar air heaters with and without fins, respectively. It is seen from the graphs that the collector efficiencies start to drop beyond mass flow rate 0.01kg/s. Moreover, it is deduced from the graphs that the collector efficiency grows slightly and steadily with increasing solar irradiance. As aforesaid, this is because more solar energy is available for the solar air heater to absorb per unit area.

4.8 Validation of The Results

In this section, the findings of the present study are evaluated in comparison with two studies overviewed in the literature. The results of the present study are validated by the findings of the investigations conducted by Rai et al. (2017) [13] and Kumar and Chand (2017) [10].

4.8.1 Temperature Rise Between Inlet and Exiting Air in Comparison to Rai et al. (2017)

The rise between the inlet and outlet air temperatures with varying mass flow rates was computed for the present study. Rai et al. (2017) [13] evaluated the temperature differences for the mass flow rates 0.0139, 0.0278, 0.0417, 0.0556, 0.0694 and 0.0833 kg/s by fixing the solar irradiance value to 750 W/m^2. In their study, they investigated how the installation of offset fins below the absorber plate affected the collector performance. The lateral spacing between the fins for both studies is 0.05 m. The fin height considered in the study of Rai et al. (2017) is 0.038 m, and 0.05 m in the present study. For a fair comparison, the temperature differences for the present study were also computed for the same mass flow rate range and solar irradiance value. Figure 27 illustrates the results of the present study and the numerical study carried out by Rai et al. (2017) [13] on the same graph.

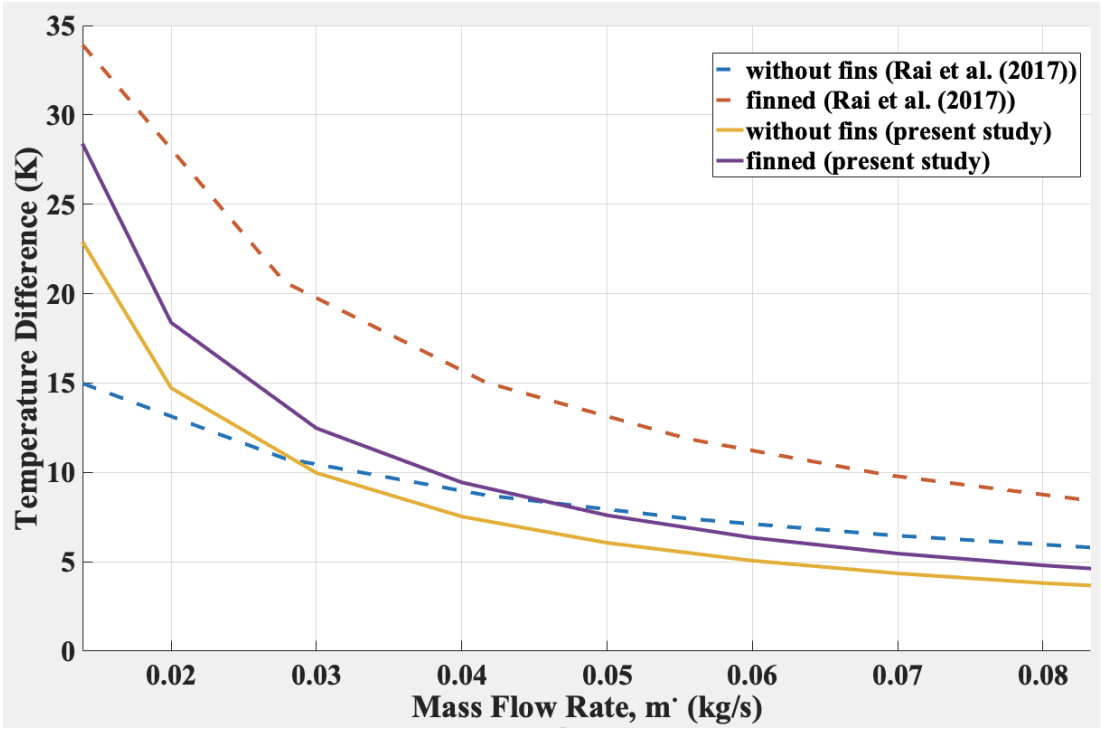

Figure 27: Temperature rise among inlet and exiting air with varying mass flow rate, at I = 750 W/m^2, in comparison to Rai et al. (2017) [13]

The numerical study of Rai et al. confirms that the finned solar heaters perform remarkably better at lower mass flow rates. For both studies, it is evaluated that the highest difference in the temperature values of the inlet and outlet air was obtained at 0.0139 kg/s. The greatest temperature difference between the inlet and exiting air for the finned solar air heater is 28.13 K and 33.92 K for present study and the investigation of Rai et al. (2017), respectively. It is observed that beyond 0.0139 kg/s, the temperature difference values start to decrease in an exponential-like fashion for the finned and conventional solar air heaters investigated in both studies. However, for the study of Rai et al. (2017), the addition of fins to the solar air heater results in a much greater rise in the exiting air temperature compared to the present study, where the rise in outlet air temperature with the addition of fins is relatively lower.

The differences in the findings of both studies is due to the fact that different fin shapes were considered; offset fins were evaluated for Rai et al. (2017), whilst rectangular fins were investigated in the present study. Another difference between the two studies is the location of where the fins were attached. For Rai et al. (2017) the fins were installed below the absorber plate, meanwhile the fins were attached to the bottom plate in the present study. Furthermore, the initial guess of the inlet temperature was 298 K for Rai et al. and 303 K for the present study. The differences in the mentioned parameters lead to differences in the results obtained.

Although there are slight differences in the findings due to the differences of some parameters, the general trend of the findings in the study of Rai et al. (2017) confirm the results of the present study. Hence, it is validated that finned solar air heaters do indeed result in an increased outlet air temperature rise compared to conventional air

heaters. Besides, it is validated that the solar air heaters perform better at lower mass flow rates.

It should be mentioned once more that this might be the opposite for other studies. For some solar air heaters, greater performance is achieved at increased mass flow rates. This is due to differences in the dimensions, arrangements and materials of the solar air heater components. These parameters affect the surface conductance, hence, some perform better at lower mass flow rates and others perform better at greater mass flow rates. Whether the solar air heater performs better at higher or lower mass flow rates depends on the surface conductance properties of the solar air heaters considered.

4.8.2 Collector Efficiency with Varying Mass Flow Rate in Comparison to Kumar and Chand (2017)

The performance of the solar air heaters with rectangular fins and no fins investigated in the present study is compared to the study carried out about how solar air heaters with herringbone fins operationally perform by Kumar and Chad (2017) [10]. Kumar and Chand tested the collector performances according to varying mass flow rates in the scope of 0.01-0.06 kg/s, by fixing the solar irradiance value to 900 W/m^2. Therefore, the same ranges were also used for the present study as it can be noticed from the graph in Figure 28.

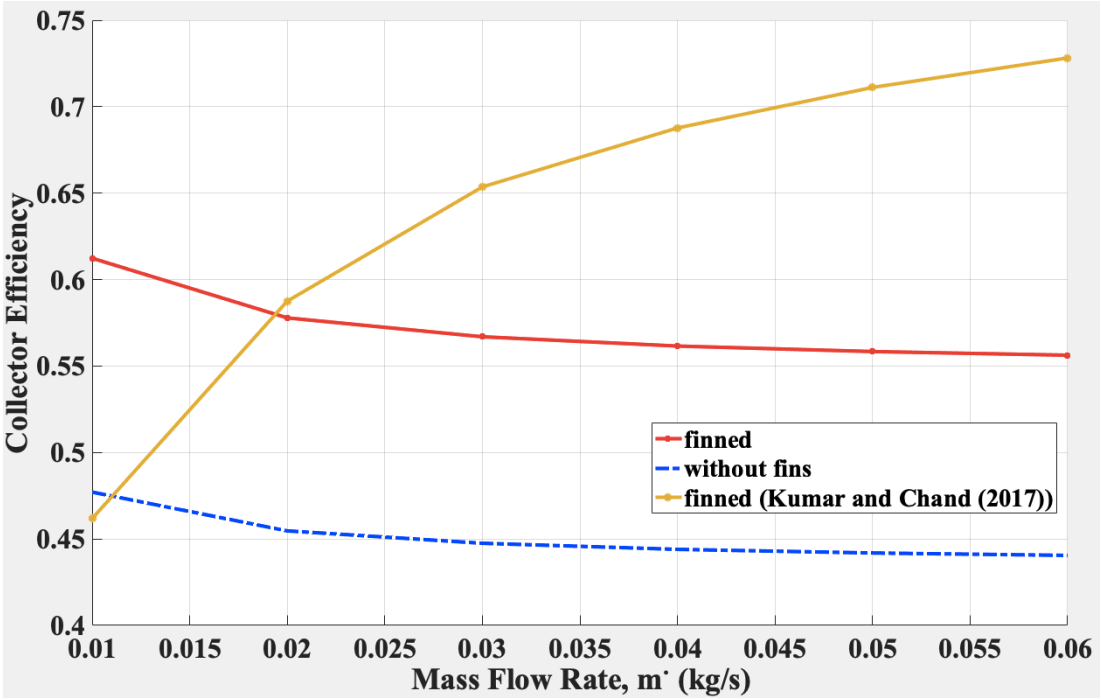

Figure 28: Collector efficiency with varying mass flow rate, I = 900 W/m^2 for present study and Kumar and Chand (2017) [10]

The solar air heater with assigned herringbone fins perform better at higher mass flow rates, whereas for the present study, the maximum performance for the finned solar air heaters is achieved at the lowest mass flow rate. This could be due to different dimensions and structural arrangements of the collector components, as well as the different fin shapes. However, the herringbone finned solar air heater still achieves greater collector efficiency values when compared to the solar air heater with no assigned fins. This confirms that finned air solar heaters perform more superiorly than conventional solar air heaters, as the results of the present study suggest. Figure 28 shows that the graph of finned solar air heater of the present study intersects with the graph of rates of the study taken from literature at mass flow rate 0.019 kg/s. This means that the differently shaped fins contribute to the enhancement of the collector performance at the same magnitude, at the mass flow rate 0.019 kg/s. The values of the collector efficiencies for the present study and the literature is provided in Table 3.

Table 3: Collector efficiency with varying mass flow rate, I = 900 W/m^2 for present study and Kumar and Chand (2017) [10].

Mass Flow Rate (kg/s)	**Efficiency (without fins, present study)**	**Efficiency (with fins, presents study)**	**Efficiency (Herringbone fins) [10]**
0.01	0.4778	0.6124	0.46180
0.02	0.4554	0.5779	0.58754
0.03	0.4482	0.5669	0.65360
0.04	0.4447	0.5616	0.68770
0.05	0.4426	0.5584	0.71114
0.06	0.4472	0.5563	0.72818

This confirms that although there may be variances in the design parameters of the solar air heaters, the addition of fins still aid in the enhancement of performance. For this case, in the study of Kumar and Chand (2017) [10] the finned solar air heater resulted in greater collector efficiencies at higher mass flow rates, whilst the opposite was true for the finned solar air heater considered in the present study. While there may be differences in the surface conductance properties of the solar air heaters considered, the results of both studies shows that regardless of the differences, finned solar air heaters perform considerably superior than conventional solar air heaters.

Chapter 5

CONCLUSIONS AND FUTURE WORKS

5.1 Conclusions

This study evaluated a comparative study between flat plate solar air heaters with fins and without fins. The aim was to investigate the impact of assigning rectangular fins on the solar air heater performance. After the analytical model based on the heat transfer fundamentals was built, it was solved numerically in an iterative manner using MATLAB-R2020b.

In brief, the finned solar air collector performed significantly better than the conventional solar air collector. This was predicted, as the inclusion of fins resulted in an increased surface area where heat transfer can take place. The finned solar air heater achieved noteworthily greater values relative to solar air heater without fins, for the heat removal factor, useful efficiency gain, outlet temperature and collector efficiency for all the tested mass flow rate and solar irradiance ranges. In the light of the results, we can, thus, draw the conclusion that assigning rectangular fins to the flat plate solar air heaters enhances the performance massively.

The solar air heaters performed better at lower mass flow rates, and relatively poorly when the mass flow rate values were at the highest. This could be due to the dimensions and the placements of the components of the solar air heaters, and how they affect the surface conductance. Some solar air heaters are expected to function better at greater

air mass flow rates, however, the findings of the present study can be confirmed by a study carried out by Rai et al. (2017) on offset fins [13]. In their study, the results indicated that the attachment of offset fins to the bottom of the absorber plate enhanced the thermal and thermohydraulic performances significantly more, at reduced mass flow rates, due to the decreased surface conductance at higher mass flow rates. Nevertheless, the finned solar air heaters tested in the present study showed a noteworthy performance across all air mass flow rate ranges.

The performance of solar air heaters were also tested for a wide range of solar irradiance values. As expected, the performance was enhanced for both of the solar air heater with increasing solar irradiance values. This could be mainly due to the fact that more solar energy could be absorbed by the collectors. The difference in the finned and non-finned performances was relatively larger for greater solar irradiance values. Hence, we could conclude that fins enhance the performance of flat plate solar air heaters especially when there of solar energy available in abundance. It is also worth to note that, despite the fact that the finned solar air heaters achieved greater collector efficiencies at higher solar irradiance values, they still performed well for lower solar intensity values. This means that the finned solar air heaters could continue to work efficiently on cloudy days, or even in geographic locations where solar energy may not be available in abundance.

Moreover, the performances of the solar air heater considered for the present study were compared to a study on herringbone fins carried out by Kumar and Chand (2017) [10]. In both studies, present and literature, the finned solar air heaters performed remarkably better than the solar air heater without fins. Hence, we can draw the conclusion that the findings of the presents study are reasonable and valid.

Lastly, it can be deduced from the results that more heat loss occurred from the front side, as opposed to the back. This is because the back of the collector was well-insulated, whilst the front side was in direct contact with the ambience. Additionally, the assigned fins helped to reduce the overall heat loss coefficients.

All things considered, it is concluded that finned solar air heaters operate significantly better than standard flat plate solar heaters, across a broad span of air mass flow rates and solar irradiances.

5.2 Future Works

The present study can be considered as a base study for future works. The present study evaluates the general behaviour of the finned and conventional solar air heaters. The impact of fins on the collector performance could be further investigated by testing the performance with fins of difference heights, thicknesses, lateral and longitudinal spacings.

Moreover, new experiments could be carried out comparing solar air heaters by altering numbers of fins attached. The location of where the fins are installed could also be altered. For the present study the fins considered were attached on the bottom plate, and in future works the attachment of fins to the absorber plate could also be tested.

REFERENCES

[1] Womac, A., Tompkins, F., & DeBusk, K. (1985). Evaluation of solar air heatersfor crop drying. *Energy In Agriculture*, *4*, 147-157. doi: 10.1016/0167-5826(85)90013-0

[2] Koyuncu, T. (2006). Performance of various design of solar air heaters for crop drying applications. *Renewable Energy*, *31*(7), 1073-1088. doi: 10.1016/j.renene.2005.05.017

[3] McVEIGH, J. (1983). Water and Air Heating Applications. *Sun Power*, *(Second Edition)*.

[4] Aravindh, M., & Sreekumar, A. (2016). Efficiency enhancement in solar air heaters by modification of absorber plate-a review. *International Journal Of Green Energy*, *13*(12), 1209-1223. doi: 10.1080/15435075.2016.1183207

[5] Chabane, F., Moummi, N., Benramache, S., Bensahal, D., & Belahssen, O. (2013). Collector Efficiency by Single Pass of Solar Air Heaters with and without Using Fins. *Engineering Journal*, *17*(3), 43-55. doi: 10.4186/ej.2013.17.3.43

[6] Yeh, H., Ho, C., & Lin, C. (1998). The influence of collector aspect ratio on the collector efficiency of baffled solar air heaters. *Energy*, *23*(1), 11-16. doi: 10.1016/s0360-5442(97)00054-6

[7] Gopi, R. (2017). Experimental investigation of flat plate collector with cylindrical fins in a solar air heater. *J. Indus Pollut Control*, *33(2)*, 1128-32.

[8] Daliran, A., & Ajabshirchi, Y. (2018). Theoretical and experimental research on effect of fins attachment on operating parameters and thermal efficiency of solar air collector. *Information Processing In Agriculture*, *5*(4), 411-421. doi: 10.1016/j.inpa.2018.07.004

[9] Mohammadi, K., & Sabzpooshani, M. (2013). Comprehensive performance evaluation and parametric studies of single pass solar air heater with fins and baffles attached over the absorber plate. *Energy*, *57*, 741-750. doi: 10.1016/j.energy.2013.05.016

[10] Kumar, R., & Chand, P. (2017). Performance enhancement of solar air heater using herringbone corrugated fins. *Energy*, *127*, 271-279. doi: 10.1016/j.energy.2017.03.128

[11] Naphon, P. (2005). On the performance and entropy generation of the double pass solar air heater with longitudinal fins. *Renewable Energy*, *30*(9), 1345-1357. doi: 10.1016/j.renene.2004.10.014

[12] Duffie, J. A., Beckman, W. A., & Worek, W. M. (1994). Solar Engineering of Thermal Processes, 2nd ed. *Journal of Solar Energy Engineering*, *116*(1), 67–68.

[13] Rai, S., Chand, P., & Sharma, S. (2017). An analytical investigations on thermal and thermohydraulic performance of offset finned absorber solar air heater. *Solar Energy*, *153*, 25–40.

[14] Ghajar, A. C. Y. A. J. (2021). *Heat And Mass Transfer, 5Ed* (5th Edition). MC GRAW HILL INDIA.

[15] Heaton, H., Reynolds, W., & Kays, W. (1964). Heat transfer in annular passages. Simultaneous development of velocity and temperature fields in laminar flow. *International Journal of Heat and Mass Transfer*, *7*(7), 763–781.

[16] Drake, R. M. (1967). W. M. Kays, Convective Heat and Mass Transfer, 387 pp. McGraw-Hill, New York (1966). *International Journal of Heat and Mass Transfer*, *10*(8), 1131–1132.

APPENDICES

Appendix A: Tables of Results Obtained

Table 4: Heat removal factors, useful energy gains, collector efficiencies with varying mass flow rates, by fixing solar irradiance at 1000 W/m^2.

m (kg/s)	FR fins	FR w/o fins	Qu fins (W)	Qu w/o fins (W)	n eff fins	n eff w/o fins
0.01	0.742841	0.57915214	613.2449267	477.8103046	0.6132	0.4478
0.02	0.700991	0.551943164	578.696129	455.362439	0.5787	0.4554
0.03	0.6877336	0.543249477	567.751558	448.1900002	0.5678	0.4482
0.04	0.6812292	0.538970662	562.381974	444.6599057	0.5624	0.4447
0.05	0.6773658	0.536424836	559.192534	442.5595562	0.5592	0.4426
0.06	0.6748063	0.534736491	557.079578	441.1666435	0.5571	0.4412
0.07	0.6729859	0.533534855	555.576815	440.1752733	0.5556	0.4402
0.08	0.671625	0.532635984	554.453279	439.4336897	0.5545	0.4393
0.09	0.670569	0.531938255	553.581506	438.8580514	0.5536	0.4389

Table 5: Useful energy obtained and collector efficiency with varying solar irradiance, $\dot{m}$ =0.01 kg/s.

I (W/m^2)	Qu fin (W)	Qu wo (W)	Efficiency fin	Efficiency w/o fin
300	178.3888	138.776958	0.5946293	0.462589861
350	209.5111	162.993626	0.5984284	0.465696074
400	240.4547739	187.210293	0.6012778	0.468025734
450	271.57226	211.426961	0.6034939	0.469837691
500	302.63341	235.643629	0.6052668	0.471287257
550	333.69456	259.860296	0.6067174	0.472473266
600	364.75571	284.076964	0.6079262	0.473461606
650	395.81686	308.293631	0.608949	0.474297895
700	426.87802	332.510299	0.6098257	0.475014713
750	457.93917	356.726967	0.6105856	0.475635956
800	489.00032	380.943634	0.6112504	0.476179543
850	520.06147	405.160302	0.611837	0.476659179
900	551.12262	429.376969	0.61213585	0.477085522
950	582.18377	453.593637	0.612825	0.477466986
1000	613.24493	477.810305	0.6132449	0.477810305
1050	644.30608	502.026972	0.6136248	0.478120926
1100	675.36723	526.24364	0.6139702	0.478403309
1150	706.42838	550.460307	0.6142856	0.478661137
1200	737.48953	574.676975	0.6145746	0.478897479

Table 6: Useful energy obtained and collector efficiency with varying solar irradiance, $\dot{m}$ = 0.02 kg/s

I (W/m^2)	Qu fin (W)	Qu wo (W)	n eff fin	n eff w/o fin
300	168.33879	132.2571188	0.5611293	0.440857063
350	197.65003	155.3360702	0.5647144	0.443817343
400	226.96127	178.4150217	0.5674032	0.446037554
450	256.2725	201.4939731	0.5694945	0.447764385
500	285.58374	224.5729245	0.5711675	0.449145849
550	314.89498	247.651876	0.5725363	0.450276138
600	344.200622	270.7308274	0.573677	0.451218046
650	373.51746	293.8097789	0.5746422	0.452015044
700	402.8287	316.8887303	0.5754696	0.452698186
750	432.13994	339.9676818	0.5761866	0.453290242
800	461.45117	363.0466332	0.576814	0.453808292
850	490.76241	386.1255847	0.5773675	0.454265394
900	520.07365	409.2045361	0.5778596	0.454671707
950	549.38489	432.2834876	0.5782999	0.45503525
1000	578.69613	455.362439	0.5786961	0.455362439
1050	608.00737	478.4413905	0.5790546	0.455658467
1100	637.31861	501.5203419	0.5793806	0.455927584
1150	666.62984	524.5992934	0.5796781	0.456173299
1200	695.94108	547.6782448	0.5799509	0.456398537

.

Table 7: Useful energy obtained and collector efficiency with varying solar irradiance, $\dot{m}$ = 0.03 kg/s.

I (W/m^2)	Qu fin (W)	Qu w/o fin (W)	n eff fin	n eff w/o fin
300	165.15509	130.1739296	0.550517	0.433913099
350	193.91198	152.8893632	0.5540342	0.436826752
400	222.66887	175.6047968	0.5566722	0.439011992
450	251.42576	198.3202305	0.5587239	0.440711623
500	280.18265	221.0356641	0.5603653	0.442071328
550	308.93954	243.7510977	0.5617083	0.443183814
600	337.69643	266.4665313	0.5628274	0.444110886
650	366.45332	289.1819649	0.5637743	0.444895331
700	395.21021	311.8973985	0.564586	0.445567712
750	423.9671	334.6128322	0.5652895	0.446150443
800	452.72399	357.3282658	0.565905	0.446660332
850	481.48089	380.0436994	0.5664481	0.447110235
900	510.23778	402.759133	0.5669309	0.447510148
950	538.99467	425.4745666	0.5673628	0.447867965
1000	567.75156	448.1900002	0.5677516	0.44819
1050	596.50845	470.9054339	0.5681033	0.448481366
1100	625.26534	493.6208675	0.568423	0.448746243
1150	654.02223	516.3363011	0.568715	0.448988088
1200	682.77912	539.0517347	0.5689826	0.449209779

Table 8: Useful energy obtained and collector efficiency with varying solar irradiance, $\dot{m}$ = 0.04 kg/s.

I (W/m^2)	Qu fin (W)	Qu w/o fin (W)	n eff fin	n eff w/o fin
300	163.59311	129.1486361	0.5453104	0.430495454
350	192.07803	151.6851554	0.5487944	0.433386158
400	220.56295	174.2216746	0.5514074	0.435554187
450	249.04787	196.7581939	0.5534397	0.437240431
500	277.53279	219.2947131	0.5550656	0.438589426
550	306.0177	241.8312324	0.5563958	0.43969315
600	334.50262	264.3677516	0.5575044	0.440612919
650	362.98754	286.9042709	0.5584424	0.441391186
700	391.47246	309.4407901	0.5592464	0.442058272
750	419.95738	331.9773094	0.5599432	0.442636413
800	448.4423	354.5138286	0.5605529	0.443142286
850	476.92722	377.0503479	0.5610908	0.443588645
900	505.41214	399.5868671	0.561569	0.443985408
950	533.89706	422.1233864	0.5619969	0.444340407
1000	562.38197	444.6599057	0.562382	0.444659906
1050	590.86689	467.1964249	0.5627304	0.444948976
1100	619.35181	489.7329442	0.5630471	0.445211767
1150	647.83673	512.2694634	0.5633363	0.445451707
1200	676.32165	534.8059827	0.5636014	0.445671652

Table 9: Useful energy obtained and collector efficiency with varying solar irradiance, $\dot{m}$ = 0.05 kg/s.

I (W/m^2)	Qu fin (W)	Qu w/o fin (W)	n eff fin	n eff w/o fin
300	162.665324	128.538603	0.54221775	0.42846201
350	190.988697	150.9686711	0.54568199	0.43133906
400	219.988697	173.3987392	0.54828017	0.433496848
450	247.635441	195.8288073	0.55030098	0.435175127
500	275.958813	218.2588754	0.55191763	0.436517751
550	304.282185	240.6889434	0.55324034	0.437616261
600	332.605557	263.1190115	0.5543426	0.438531686
650	360.928929	285.5490796	0.55527528	0.439306276
700	389.252302	307.9791477	0.55607472	0.439970211
750	417.575674	330.4092158	0.55676756	0.440545621
800	445.899046	352.8392839	0.55737381	0.441049105
850	474.222418	375.269352	0.55790873	0.441493355
900	502.54579	397.69942	0.55838421	0.441888244
950	530.869162	420.1294881	0.55880964	0.442241566
1000	559.192534	442.5595562	0.55919253	0.442559556
1050	587.515906	464.9896243	0.55953896	0.442847261
1100	615.839279	487.4196924	0.55985389	0.443108811
1150	644.162651	509.8497605	0.56014144	0.443347618
1200	672.486023	532.2798285	0.56040502	0.443566524

Table 10: Useful energy obtained and collector efficiency with varying solar irradiance, $\dot{m}$ = 0.06 kg/s.

I (W/m^2)	Qu fin (W)	Qu w/o fin (W)	n eff fin	n eff w/o fin
300	162.05068	128.1340404	0.54016893	0.427113468
350	190.267029	150.4935121	0.54362008	0.429981463
400	218.483379	172.8529837	0.54620845	0.432132459
450	246.699729	195.2124554	0.54822162	0.433805456
500	274.916079	217.571927	0.54983216	0.435143854
550	303.132429	239.9313987	0.55114987	0.436238907
600	331.348779	262.2908703	0.55224796	0.437151451
650	359.565129	284.650342	0.55317712	0.437923603
700	387.781478	307.0098136	0.55397354	0.438585448
750	415.997828	329.3692853	0.55466377	0.439159047
800	444.214178	351.7287569	0.55526772	0.439660946
850	472.430528	374.0882286	0.55580062	0.440103798
900	500.636878	396.4477002	0.55627431	0.440497445
950	528.863228	418.8071719	0.55669813	0.440849655
1000	557.079578	441.1666435	0.55707958	0.441166644
1050	585.295927	463.5261152	0.55742469	0.441453443
1100	613.512277	485.8855868	0.55773843	0.44171417
1150	641.728627	508.2450585	0.55802489	0.441952225
1200	669.944977	530.6045301	0.55828748	0.442170442

Table 11: Useful energy obtained and collector efficiency with varying solar irradiance, $\dot{m}$ = 0.07 kg/s.

I (W/m^2)	Qu fin (W)	Qu w/o fin (W)	n eff fin	n eff w/o fin
300	161.613536	127.8461032	0.53871179	0.426153677
350	189.75377	150.1553297	0.54215363	0.429015228
400	217.894005	172.4645561	0.54473501	0.43116139
450	246.034239	194.7737825	0.54674275	0.432830628
500	274.174475	217.083009	0.54834895	0.434166018
550	302.314707	239.3922354	0.5496631	0.43525861
600	330.454942	261.7014618	0.55075824	0.436169103
650	358.59176	284.0106883	0.55168489	0.43693952
700	386.73541	306.3199147	0.55247916	0.437599878
750	414.875644	328.6291411	0.55316753	0.438172188
800	443.015878	350.9383676	0.55376985	0.438672959
850	471.156113	373.247594	0.55430131	0.439114816
900	499.296347	395.5568204	0.55477372	0.439507578
950	527.436581	417.8660469	0.5551964	0.439858997
1000	555.576815	440.1752733	0.55557682	0.440175273
1050	583.717049	462.4844997	0.555921	0.440461428
1100	611.857284	484.7937262	0.55623389	0.440721569
1150	639.997518	507.1029526	0.55651958	0.440959089
1200	668.137752	529.4121791	0.55678146	0.441176816

Table 12: Useful energy obtained and collector efficiency with varying solar irradiance, $\dot{m}$ = 0.08 kg/s.

I (W/m^2)	Qu fin (W)	Qu w/o fin (W)	n eff fin	n eff w/o fin
300	161.286707	127.630715	0.53762236	0.42543572
350	189.370034	149.9023561	0.54105724	0.42829245
400	217.45336	172.1739971	0.5436334	0.43043499
450	245.536687	194.4456382	0.54563708	0.43210142
500	273.620013	216.7172792	0.54724003	0.43343456
550	301.70334	238.9889202	0.54855153	0.43452531
600	329.786667	261.2605613	0.54964444	0.43543427
650	357.869993	283.5322023	0.55056922	0.43620339
700	385.95332	305.8038434	0.55136189	0.43686263
750	414.036646	328.0754844	0.55204886	0.43743398
800	442.119973	350.3471255	0.55264997	0.43793391
850	470.203299	372.6187665	0.55318035	0.43837502
900	498.286626	394.8904076	0.55365181	0.43876712
950	526.369953	417.1620486	0.55407363	0.43911795
1000	554.453279	439.4336897	0.55445328	0.43943369
1050	582.536606	461.7053307	0.55479677	0.43971936
1100	610.619932	483.9769718	0.55510903	0.43997907
1150	638.703259	506.2486128	0.55539414	0.44021619
1200	666.786585	528.5202539	0.55565549	0.44043354

Table 13: Useful energy obtained and collector efficiency with varying solar irradiance, $\dot{m}$ = 0.09 kg/s.

I (W/m^2)	Qu fin (W)	Qu w/o fin (W)	n eff fin	n eff w/o fin
300	161.033114	127.4635245	0.53677705	0.424878415
350	189.072285	149.7059908	0.54020653	0.427731402
400	217.111456	171.948457	0.54277864	0.429871142
450	245.150627	194.1909232	0.54477917	0.431535385
500	273.189798	216.4333894	0.5463796	0.432866779
550	301.228969	238.6758556	0.54768903	0.433956101
600	329.26814	260.9183218	0.54878023	0.43486387
650	357.30731	283.160788	0.54970355	0.435631982
700	385.346481	305.4032542	0.55049497	0.436290363
750	413.385652	327.6457204	0.55118087	0.436860961
800	442.424823	349.8881866	0.55178103	0.437360233
850	469.463994	372.1306528	0.55231058	0.437800768
900	497.503165	394.373119	0.55278129	0.438192354
950	525.542336	416.6155852	0.55320246	0.438542721
1000	553.581506	438.8580514	0.55358151	0.438858051
1050	581.620677	461.1005176	0.55392445	0.43914335
1100	609.659848	483.3429839	0.55423623	0.439402713
1150	637.699019	505.5854501	0.55452089	0.439639522
1200	665.73819	527.8279163	0.55478182	0.439856597

Appendix B: Snippets of The Code Developed in MATLAB

```
hw = (8.6*(V^0.4))/(Lc^0.4); %same as glass-ambient convective heat
transfer
h_rga = Eg* G*(Tg - Ta)*((Tg^2)-(Ta^2)) ; %radiative heat transfer
glass- ambinet
h_rpg = (G * (Tp+Tg)*((Tp^2)+(Tg^2)))/((1/Ep)+(1/Eg)-1); %rad
absorber plate and glass cover
h_r = (G * (Tp+Tb)*((Tp^2)+(Tb^0.5)))/((1/Ep)+(1/Eb)-1); %rad
absorber plate- bottom %remember h_rpb*****
ka = (0.0015215+(0.097459*Tf)-(3.3322e-5 *(Tf^2)))* 0.001; %air
thermal conduct
cp = 999.2 + (0.1434*Tf) + (1.101e-4 *(Tf^2))-(6.7581e-8 *(Tf^3));
%usually equivalent to 1000 J/kgK
u = (1.6157e-6 + (0.06523e-6 *Tf) -(3.0297e-11 * (Tf^2)));
p = (3.9147 - (0.016082* Tf) + (2.9013e-5 *(Tf^2) - (1.9407e-8 *
(Tf^0.3))));
Pr = (u * cp)/ka ; %Prandtl number is calculated
T = (Tp+Tg)/2; %mean of glass and absorber
B = 1/T;
Ra = ((g*B*Pr)/(v^2))*(Tp-Tg)*(dpg)^0.3;
Nupg = 1+1.44*(1- ((1708/(Ra* cos(theeta)))* (1 -
((1708*((sin(1.8*theeta))^1.6))/(Ra*cos(theeta))))+((((Ra*cos(theeta
))/5830)^0.333)-1)));
hc_pg = Nupg *(ka/dpg);
Dh_wo = (2*B*H)/(B+H); %hydraulic diameter
Dh_fin = (4*((B*H)-(Lt*Wt*Nti)))/(2*(B+H+(Lt*Nti))); %hydraulic
diameter with fins
Re_wo = (p*V*Dh_wo)/u; %reynolds number calculation for SAH without
fins ***** check if turbulent or laminar****
Re_fin = (p*V*Dh_fin)/u; % reynold no calc for SAH with fins
****check if turbulent ot laminar****
%%% if reynolds number shows the flow is laminar use this:
% Nu = 4.4 +
% ((0.00398*(0.7*Re*(Dh/Lc))^1.66/(1+(0.0114*(0.7*Re(Dh/Lc))^1.12)
% ******remember to add _fin and _wo where appropriate*******
Nu_fin = 0.0158*(Re_fin)^0.8; % nusselt number finned
Nu_wo = 0.0158*(Re_wo)^0.8; %nusselt number wo fins
%h1_fin = (ka/Dh_fin)* Nu_fin; % =h2 = hc (remember to use
interchangeably)%% hc_pa
h1 = (ka/Dh_wo)*Nu_wo; % =h2 = hc (remember to use interchangeably)
%%hc_pa %%initially h1_wo
M  = sqrt ((2*h1_fin)/(ka*tf));
nfin = ((tanh(M*Lt)))/(M*Lt); %fin EFFECTIVE efficiency (for the fin
only)
phi = 1 + (Af/Ac)*nfin;
f = (1-(0.004*hw) + (0.0005*(hw^2)))*(1+(0.091*Ng)); %%for front
side calculations
C = 365.9 * (1 -(0.0083*theeta)+(0.0001298*(theeta^2))); %%for front
side calculations
Ut = (Ng/((C/Tp)*((Tp-Ta)/Ng+f)^0.33 +(1/hw))^-1 + ((G*(Tp-
Ta)*((Tp^2)-(Ta^2)))/((1/(Ep+((0.05*Ng)*(1-Eg))))+(((2*Ng)+f-1)/Ep)-
1)));
Ub = ks/ds;
UL_wo = Ut+ Ub;
UL_fin =
((Ub+Ut)*((h1*h1*phi)+(h1*h_r))+(h1*phi*h_r)+((Ub*Ut)*(h1+h1*phi)))/
((h1*h_r)+(h1*phi*Ut)+(h1*phi*h_r)+(h1*h1*phi));
%remember that h1 and h2 are used interchangeably*******
h= h1 +(1/((1/h1)+(1/h_r)));
F_wo = h/(h+UL);    %%efficiency FACTOR (not efficiency)
```

```
F_fin =
((h_r*h1)+(h1*phi*Ut)+(h1*phi*h_r)+(h_r*h1*phi))/((Ut+h_r+h1)*(Ub+(h
1*phi)+h_r)-(h_r^0.2)); %%effiency FACTOR (not efficiency)
T_a_e = (1.01 * tau* alpha); %% calculate for effective trasmitted
absorption coeff

%%% TO CHECK FOR TEMPERATURES******
% note:DIFFERENCE (NEW-GUESS) MUST BE LESS THAN OR EQUAL TO 0.001
%Tg = ((alpha*I)+Tp*(hc_pg +
h_rpg)+Ta*(hw+h_rga))/(hc_pg+h_rpg+h_rga); %glass plate temperature
NEW
%Tp = ((alpha*I*tau)+Tg(hc_pg+h_rpg)+(Tb*h_r)+
(Tf*h1))/(hc_pg+h_rpg+h_r+h1); %absorber plate temperature NEW
%Tb = ((Tp*h_r)+(Tf*phi*h1)+(Ta*Ub))/((h_rpb)+(phi*h1)+Ub); %bottom
plate plate temperature NEW
%Tf = ((Ti*m*cp)+(Tp*h1)+(Tb*phi*h1))/((m*cp)+h1+(phi*h1));


%For mass flow rate m =0.01 kg/s (rearranged the equations above and
%substituted appropriate values)
 syms Tg Tp Tb Tf

equation1 = 10.0907*Tp ==2664.785775;
equation2 = 10.0907*Tg + 7.02*Tb + 13.28*Tf == 9600.568705
equation3 = 7.02*Tp + 14.523*Tf == 7091.973075;
equation4 = 13.28*Tp +14.523*Tb ==8424.311424;
sol = solve ([equation1, equation2, equation3, equation4],[Tg, Tp,
Tb, Tf]);
Tgsol = sol.Tg;
Tpsol = sol.Tp;
Tbsol = sol.Tb;
Tfsol = sol.Tf;

%check for difference

Tg - Tg_guess
Tp - Tp_guess
Tb - Tb_guess
Tf - Tf_guess

%****Outputs after iterative method*****

S = T_a_e * I;

FR_fin = (((m.*cp)./(Ac.*UL_fin)).*(1-
(exp((Ac.*UL_fin.*F_fin)./(m.*cp)))))
FR_wo = (((m.*cp)./(Ac.*UL_wo)).*(1-
(exp((Ac.*UL_wo.*F_wo)./(m.*cp)))))

Qu_fin = ((Ac.*FR_fin).*(S-(UL_fin .*(Ti - Ta))))
Qu_wo = ((Ac.*FR_wo).*(S-(UL_wo .*(Ti - Ta))))

n_eff_fin = Qu_fin./(Ac.*I)
n_eff_wo = Qu_wo./(Ac.*I)

T0_fin = Ti +((1./UL_fin).*(S -(UL_fin.*(Ti-Ta))).*(1-exp((-
Ac.*UL_fin.*F_fin)./(m.*cp))))
T0_wo = Ti +((1./UL_wo).*(S -(UL_wo.*(Ti-Ta))).*(1-exp((-
Ac.*UL_wo.*F_wo)./(m.*cp))))
```